Engineering Structures 202 (2020) 109888

Contents lists available at ScienceDirect

Engineering Structures

journal homepage: www.elsevier.com/locate/engstruct

Drying shrinkage model for recycled aggregate concrete accounting for the influence of parent concrete

Qinghe Wang[a], Yue Geng[b,c,d,*], Yuyin Wang[b,c,d], Huan Zhang[d]

[a] School of Civil Engineering, Shenyang Jianzhu University, 9 Hunnan Rd., Shenyang 110168, Liaoning, China
[b] Key Lab of Structures Dynamic Behaviour and Control of the Ministry of Education, Harbin Institute of Technology, Harbin 150090, China
[c] Key Lab of Smart Prevention and Mitigation of Civil Engineering Disasters of the Ministry of Industry and Information Technology, Harbin Institute of Technology, Harbin 150090, China
[d] School of Civil Engineering, Harbin Institute of Technology, Heilongjang, Harbin 150090, China

ARTICLE INFO

Keywords:
Recycled aggregate concrete
Drying shrinkage model
Recycled coarse aggregate
Parent concrete
Residual mortar

ABSTRACT

The drying shrinkage of recycled aggregate concrete (RAC) varies considerably owing to the extensive sources of parent concrete from which recycled aggregates are obtained. This paper proposes a theoretical drying shrinkage model for RAC considering the properties of the parent concrete, including its service time and strength. To achieve this, shrinkage tests were conducted on 60 concrete specimens over 360 days. Five types of parent concrete with different service times (1 year, 20 years, and 42 years) and water-to-cement ratios (0.30, 0.45, and 0.60) were crushed to obtain recycled coarse aggregates (RCAs) that were used to prepare the RAC specimens. Three RCA replacement ratios (0%, 50%, and 100%) and three RAC water-to-cement ratios (0.30, 0.45, and 0.60) were assessed. The results indicated that the drying shrinkage of RAC was effectively reduced by an increase in the parent concrete strengths and vice versa. A theoretical RAC shrinkage model was developed considering the influence of the residual mortar content and parent concrete strength. A benchmarking analysis using 262 shrinkage samples demonstrated that the proposed model offers improved accuracy for estimating the long-term drying shrinkage of RAC over existing methods, particularly when the parent concrete and RAC have large strength variations.

1. Introduction

Recycled aggregate concrete (RAC), which uses aggregates from waste concrete (known as parent concrete), has significant environmental and economic benefits [1–4]. After crushing, the mortar from the parent concrete remains adhered to the original virgin aggregate (OVA), and consequently the recycled coarse aggregates (RCAs) have worse basic properties than conventional aggregates [5–12]. RCAs are generally recommended for use in non-structural members, although a few design specifications have recommended the use of RAC in reinforced concrete structures, with clearly defined RCA physical qualities, applied compressive strength, maximum replacement ratios, etc. [13–17]. Over the past three years, two specifications of RAC composite structures have been issued in China to further promote their commercial applications [18,19].

Extensive research on the mechanical behaviour of RAC exists. The basic properties of RCAs and RAC were initially believed to be highly dependent on the residual mortar [20–22]. However, the residual mortar content and quality are significantly influenced by the size of the OVA and RCA [23], parent concrete strength [24–27], service time of parent concrete [28], etc. At the aggregate level, researchers have attempted to establish a relationship between the residual mortar content (C_{RM}) and the basic properties of RCAs, such as density, water absorption, and Los Angeles abrasion [5,29–31], and recommended optimal values of residual mortar content for structural applications of RCAs [5]. At the concrete level, experimental studies to investigate the influence of C_{RM} on the basic properties of RAC, such as the compressive strength [32–34], tensile strength [35–37], elastic modulus [37,38], and creep [39,40] were conducted, and revealed that the properties of RAC degraded with the increase in C_{RM}. To predict these mechanical properties, regression analysis was initially used to account for the RCA replacement (r) ratio [41,42], however, the accuracy of regressed models depends on the scale of the database. Subsequently theoretical models that predict the compressive strength [43,44], tensile strength [38], elastic modulus [37,38], and creep [45] of RAC using two-phase composite material theory, i.e. treating the RCAs as a

* Corresponding author at: School of Civil Engineering, Harbin Institute of Technology, PO Box 2551, 73 Huanghe Road, Harbin 150090, China.
E-mail addresses: wangqinghe@sjzu.edu.cn (Q. Wang), gengyue@hit.edu.cn (Y. Geng), wangyuyin@hit.edu.cn (Y. Wang), zhanghuan916@hit.edu.cn (H. Zhang).

https://doi.org/10.1016/j.engstruct.2019.109888
Received 14 May 2019; Received in revised form 1 November 2019; Accepted 3 November 2019

Nomenclature

CA	coarse aggregate
COV	coefficient of variation
ITZ	interfacial transition zone
NAC	natural aggregate concrete
NCA	natural coarse aggregate
NFA	natural fine aggregate
NM	natural mortar
OVA	original virgin aggregate
PC	parent concrete
RAC	recycled aggregate concrete
RCA	recycled coarse aggregate
RM	residual mortar
SP	superplasticiser
SSD	saturated surface-dried
a, b, c	coefficients used in the drying shrinkage model
C_{RM}	residual mortar content of RCA
D_{NAC}	weighted density of aggregates in NAC
D_{RAC}	weighted density of aggregates in RAC
E_c	elastic modulus of concrete
E_c^{PC}	elastic modulus of parent concrete
f_{cm}	compressive strength of concrete
f_{cm}^{PC}	compressive strength of parent concrete
f_{cm}^{NAC}	compressive strength of NAC
f_{cm}^{RAC}	compressive strength of RAC
n	empirical coefficient in the drying shrinkage model
r	replacement ratio of RCA
R_H	relative humidity
S	service time of parent concrete
T	temperature
V_{NCA}^{NAC}	volume fraction of NCA in NAC
V_{NM}^{NAC}	volume fraction of natural mortar (NM) in NAC
V_{NCA}^{RAC}	volume fraction of NCA in RAC
V_{RM}^{RAC}	volume fraction of residual mortar (RM) in RAC
V_{TNCA}^{RAC}	total volume fraction of NCA in RAC
V_{TM}^{RAC}	total volume fraction of mortar in RAC
V_{OVA}^{RAC}	volume fraction of original virgin aggregate (OVA) in RAC
V_{CA}^{RAC}	volume fraction of coarse aggregate (CA) in RAC
Wa_{NAC}	weighted water absorption of aggregates in NAC
Wa_{RAC}	weighted water absorption of aggregates in RAC
w/b	water-to-binder ratio of concrete
w/c	water-to-cement ratio of concrete
w_{or}/c_{or}	original water-to-cement ratio of parent concrete
ε_{sh}	drying shrinkage of concrete
$\varepsilon_{sh,360}$	drying shrinkage of concrete at 360 days
ε_{sh}^{NAC}	drying shrinkage of NAC
ε_{sh}^{NM}	drying shrinkage of natural mortar (NM)
ε_{sh}^{RAC}	drying shrinkage of RAC
ε_{sh}^{TM}	drying shrinkage of new and residual mortar ensemble in RAC
$\kappa_{sh,a}$, $\kappa_{sh,f}$	shrinkage coefficients caused by the volume change of coarse aggregate in recycled concrete, and by the difference in the drying shrinkage properties of natural mortar and residual mortar
κ_{sh}	drying shrinkage amplification factor

combination of residual mortar (RM) and OVA, have been proposed. Recently, researchers have reported that creep models that include C_{RM} cannot provide reasonable estimations for high-strength RAC (lower w/c ratios) or RAC using RCAs from high-strength parent concrete. Efforts have since been made to include the effect of parent concrete properties in the prediction models [8,46].

In addition to above-mentioned mechanical properties, long-term drying shrinkage deformation is an important control factor in the overall design of RAC when introduced to structural members [47–49]. Ravindrarajah and Tam (1985) [26] measured the drying shrinkage of RAC, with a test period of 70 days and an r ratio of 100%, and obtained an increase in drying shrinkage of up to 95%. Subsequently, researchers partially replaced natural coarse aggregates (NCAs) with RCAs to prepare normal-strength and high-strength RAC with w/c ratios of 0.26–0.75 [50–60], and evaluated their shrinkage behaviour. The results indicated that RAC of varying strengths (w/c ratios) exhibited higher drying shrinkage with the increase in RCA r ratios. However, these increases varied significantly, ranging from 0.1% to 121.3% [61]. This was attributed to the extensive sources of RCAs, each possessing different characteristics. For example, de Brito et al. (2011) [62,63] reported that the RAC drying shrinkage significantly increased with the degradation of the physical properties of RCAs (i.e. RCA density and water absorption), and Duan and Poon (2014) [20] observed that the RAC drying shrinkage increased with the increase in the residual mortar content of RCAs. Besides the above-mentioned factors, the residual mortar quality (primarily determined by the service time and strength of parent concrete) may also influence the drying shrinkage of RAC, although different conclusions have been reported to date. Katz [64] selected three types of young parent concrete specimens with different service times (1, 3, and 28 days), to prepare RAC with r = 100%. The results showed that the RAC specimen made with RCAs crushed after 28 days had the largest 90-day drying shrinkage. Kou and Poon [25], Gonzalez-Corominas and Etxeberria [59], and Gholampour and Ozbakkaloglu [65] reported that RCA from higher-strength parent concrete could help reduce the drying shrinkage of resulting concrete, while Pedro et al. (2014) [66] reported that parent concrete strength had no significant impact on the drying shrinkage of resulting concrete. Several expressions predicting the drying shrinkage of RAC have been proposed based on these experiments. While Seara-Paz reported that RAC demonstrated a relatively smaller early age total shrinkage than NAC due to the inner curing effects on autogenous shrinkage [47,67], others have suggested that both NAC and RAC have similar trends of the development of drying shrinkage [8,68–70]. Most researchers tend to establish an approximate relationship between the RAC drying shrinkage and the reference NAC drying shrinkage using a shrinkage amplification factor (κ_{sh}). Initially, only the RCA replacement (r) ratio was selected as a key parameter [61,71], as adopted by current design specifications [17]. Subsequently, weighted aggregate water absorption ratio (Wa_{RAC}/Wa_{NAC}) or weighted aggregate density ratio (D_{RAC}/D_{NAC}) and C_{RM} have also been introduced to further refine the drying shrinkage models [62,63]. Despite these improvements, large variations in the predicted shrinkage amplification factor (κ_{sh}) have been reported [72]. Further research is required to accurately predict the drying shrinkage of RAC, by following the research approaches adopted in the creep models of RAC [8,46]. The studies discussed above indicate that the source of parent concrete may influence the drying shrinkage of the RAC. However, very little effort has been devoted to quantifying the influence of the strength and the service time of parent concrete on the drying shrinkage of RAC.

2. Objectives

The aim and objective of this study is to theoretically propose drying shrinkage model for recycled aggregate concrete (RAC) accounting for the properties of parent concrete, including its service time and strength. This is achieved using two-phase composite models, in which the recycled coarse aggregate (RCA) is treated as the compositions of original virgin aggregate (OVA) and residual mortar (RM). Only a few parameters in the newly proposed model need to be regressed using the test results collected from this study, and therefore this model

is expected to have better accuracy with wider parameter ranges, compared with available drying shrinkage models that are directly regressed based on limited test data. For this purpose, parent concretes with varied water-to-cement ratios are systemically prepared to quantify the influence of parent concrete strength on the drying shrinkage of resulting RAC; and parent concretes with service time older than 1 year are collected from real projects to further investigate the impact of the service time of parent concrete on the RAC drying shrinkage, as in practice RCAs are usually stored for a quite long time before used in structural applications. Based on the experiment results collected from this study and those available in literature, a modified shrinkage model is theoretically derived accounting for the influence of parent concrete, by "$\kappa_{sh,a}$" to consider the influence of residual mortar content (C_{RM}) and by "$\kappa_{sh,f}$" to account for the difference in the shrinkage behaviour between residual mortar and natural mortar.

3. Experimental program

The details of the long-term shrinkage specimens are listed in Table 1. The variables investigated in this study were the RCA replacement ratio (r), service time of parent concrete (S), original water-to-cement ratio of parent concrete (w_{or}/c_{or}) and water-to-cement ratio of resulting concrete (w/c). Particularly, a total 20 batches of RAC were designed with RCA r ratios of 0%, 50%, and 100%, and with new water-to-cement (w/c) ratio of 0.30, 0.45 and 0.60. Three groups of parent concrete were collected from a laboratory with a service time of 1 year, and had original water-to-cement ratio (w_{or}/c_{or}) of 0.30, 0.45 and 0.60. Another two groups of parent concrete were also sourced from real demolitions with service times of 20 years and 42 years, and had original water-to-cement ratio (w_{or}/c_{or}) of 0.45. The compressive strength and elastic modulus of concrete were measured at 28 days and 90 days, and drying shrinkage was monitored for a test period of 360 days.

3.1. Materials

Portland cement (CEM 42.5 N) was used as the binder in the concrete mixture. River sand (0–5 mm) with a fineness modulus of 2.58 and crushed Andesite (5–25 mm) were used as the natural fine aggregate (NFA) and natural coarse aggregate (NCA), respectively, both of which are representative aggregate sources widely used in concrete mixtures across China. Superplasticiser (SP) AS-I with a density of 1200 kg/m^3 was added to the mix to provide enough workability to the concrete mixes.

The parent concretes prepared in laboratory and from real demolition projects were used in this study, whose mixes ingredients and mechanical properties are reported in Table 2. Particularly, three groups of parent concrete with w_{or}/c_{or} ratios of 0.30, 0.45, and 0.60 were poured into 1000 mm × 1000 mm × 120 mm mould in laboratory and cured for a time period of 1 year before crushed. The curing conditions could represent typical indoor condition in the northeast of China (e.g. [72]). Their mechanical properties were measured by means of companion material cubes and prisms. The 20- and 42-year-old parent concretes were sourced from real demolition projects with the w/c ratio of 0.45, and their 28-day compressive strength and elastic modulus values were provided in the construction documentation. These two demolished buildings represent typical structures adopting normal strength concrete and demolished after their service lives. The five groups of parent concrete underwent a two-stage crushing process to achieve a proper size fraction conforming to JGJ-52-2006 [73], with a particle size of 5–25 mm. From here on, the three groups of RCAs from the laboratory parent concrete with a service time of 1 year are referred to as RCA-S1-H, RCA-S1-M, and RCA-S1-L, wherein 'S1' denotes the service time of 1 year and 'H', 'M', and 'L' denote the w_{or}/c_{or} levels, i.e. high w_{or}/c_{or}, medium w_{or}/c_{or}, and low w_{or}/c_{or}, respectively. Similarly, the other two groups of RCAs are from real-world projects, with a service time of 20 years and 42 years and medium w_{or}/c_{or}, and are referred to as RCA-S20-M and RCA-S42-M.

Similar particle size distributions were specified for the coarse aggregates, i.e. RCA and NCA, as listed in Table 3. The basic properties of the aggregates according to JGJ-52-2006 [73], i.e. oven-dried density, surface saturation density, water absorption, and index of crushing, are also listed in Table 3. The value of each basic property listed in Table 3 is the average measurement of three identical samples. The residual mortar content of the RCA (C_{RM}) was measured using a thermal

Table 1
Details of specimens for drying shrinkage tests.

Notation	Mix designation [a]	Type of RCA	r (%)	Parent concrete properties[b]		
				S (year)	w_{or}/c_{or}	f_{cm}^{PC}(MPa)
Series L: w/c = 0.30	NCA-L	–	0	–	–	–
Low w/c concrete	RCA-S42-M-50-L	RCA-S42-M	50	42	0.45	40.2
	RCA-S42-M-100-L	RCA-S42-M	100	42	0.45	40.2
	RCA-S1-L-100-L	RCA-S1-L	100	1	0.30	62.7
	RCA-S1-M-100-L	RCA-S1-M	100	1	0.45	44.2
	RCA-S1-H-100-L	RCA-S1-H	100	1	0.60	36.9
Series M: w/c = 0.45	NCA-M	–	0	–	–	–
Medium w/c concrete	RCA-S42-M-50-M	RCA-S42-M	50	42	0.45	40.2
	RCA-S42-M-100-M	RCA-S42-M	100	42	0.45	40.2
	RCA-S20-M-50-M	RCA-S20-M	50	20	0.45	40.2
	RCA-S20-M-100-M	RCA-S20-M	100	20	0.45	40.2
	RCA-S1-L-100-M	RCA-S1-L	100	1	0.30	62.7
	RCA-S1-M-100-M	RCA-S1-M	100	1	0.45	44.2
	RCA-S1-H-100-M	RCA-S1-H	100	1	0.60	36.9
Series H: w/c = 0.60	NCA-H	–	0	–	–	–
High w/c concrete	RCA-S42-M-50-H	RCA-S42-M	50	42	0.45	40.2
	RCA-S42-M-100-H	RCA-S42-M	100	42	0.45	40.2
	RCA-S1-L-100-H	RCA-S1-L	100	1	0.30	62.7
	RCA-S1-M-100-H	RCA-S1-M	100	1	0.45	44.2
	RCA-S1-H-100-H	RCA-S1-H	100	1	0.60	36.9

[a] For the nomenclature, the concrete specimen was named by "Aggregate type-Replacement ratio-Concrete w/c level". Using 'RCA-S42-M-50-L' for example, RCA-S42-M denotes that recycled aggregate are sourced from parent concrete with service time of 42 years and medium original water-to-cement ratio (w_{or}/c_{or}); 50 is the RCA replacement ratio of 50%; the following L stands for low w/c level of resulting concrete.
[b] S, w_{or}/c_{or} and f_{cm}^{PC} is the service time, original water-to-cement ratio and compressive strength of parent concrete.

Table 2
Mechanical properties of parent concrete.

Parent concrete source	Aggregate	Mix proportions (kg/m^3)					w_{or}/c_{or}	S (year)	f_{cm}^{PC} (MPa)	E_c^{PC} (GPa)
		Water	Cement	NFA	NCA	SP				
Laboratory concrete	RCA-S1-L	180	600	610	1080	6.0	0.30	1	62.7	34.0
	RCA-S1-M	180	400	670	1180	4.0	0.45	1	44.2	31.2
	RCA-S1-H	180	300	710	1240	3.0	0.60	1	36.9	27.3
Real demolition concrete	RCA-S20-M	180	400	N/A	N/A	N/A	0.45	20	40.2	30.2
	RCA-S42-M	180	400	N/A	N/A	N/A	0.45	42	40.2	30.5

Note: SP stands for superplasticiser; w_{or}/c_{or} and S is the original water-to-cement ratio and service time of parent concrete; f_{cm}^{PC} and E_c^{PC} is the compressive strength and elastic modulus of parent concrete measured on 100 mm^3 cubes and 150 × 150 × 300 mm^3 prisms, respectively.

treatment method [5,20]. As listed in Table 3, the five types of RCAs had similar physical properties, with a maximum difference of 11.0% in water absorption and 4.1% in oven-dried density, despite exhibiting significantly different C_{RM} values. This suggests that in addition to the residual mortar content, mortar compactness may also influence the physical properties of RCAs.

3.2. Concrete mixtures

Three series of concrete mixtures, i.e. Series L (low *w/c* of 0.30), Series M (medium *w/c* of 0.45), and Series H (high *w/c* of 0.60), were prepared using NCA and the five groups of RCAs (Table 4). The *w/c* ratios were determined according to JGJ-55-2011 [74], which recommends *w/c* ratios of 0.40–0.70 for normal-strength natural concrete, and *w/c* ratios of 0.24–0.33 for high-strength natural concrete. A *w/c* ratio of around 0.30 could also be obtained from similar studies on high-strength recycled concrete–0.28 in [23] and 0.26 in [68,69]. In this study, the sand ratio and water content were equal for the NAC and the RAC at 0.36 and 180 kg/m^3, respectively. The RCA content was determined by replacing a fraction of the NCA by weight, i.e. 50% and 100%. A total of 20 batches of concrete were prepared, with three identical samples designed for each measurement. For each concrete batch, six 100 mm-cubes and six 150 mm × 150 mm × 300 mm-prisms were cast to measure the compressive strength at 28 and 90 days and elastic modulus at 28 and 90 days, respectively. Furthermore, three 100 mm × 100 mm × 400 mm-prisms were cast to measure the drying shrinkage.

For the mixing procedures used in this test, the RCAs were designed in a saturated surface-dry (SSD) condition, and this was achieved by pre-soaking the RCAs in water tank for 24 h before draining it for approximately 1 h [8–10]. Other mixing procedures could be obtained from our previous studies [8–10]. Concrete workability was measured with the slump test and the slump values were maintained in the ranges of (110 ± 20) mm, (180 ± 20) mm, and (150 ± 20) mm for Series L (low *w/c* concrete), Series M (medium *w/c* concrete), and Series H (high *w/c* concrete), respectively.

3.3. Test methods

The cubes and prisms were cured in the laboratory for 24 h, after sealing their top surface with aluminium foil (ambient environmental temperature of about 23 °C), before being demoulded. They were then wet-cured until their corresponding test ages. A 2000 kN compression machine was used to obtain the compressive strength of the concrete specimens. The loading rates in the compressive tests were 5.0 kN/s, in accordance with the requirements of GB/T 50081-2002 [75] and BS EN 12390 [76]. The elastic modulus of concrete was determined according to GB/T 50081-2002 [75] and UNI EN 83316 [77] using the same compression machine.

The drying shrinkage over time was measured in accordance with GB/T 50082-2009 [78] and ASTM C157 [79]. Demec gauges, 200 mm in length, were used to measure the shrinkage of the prisms. The prisms were first immersed in a water tank for 28 days, and their initial lengths were measured. Subsequently, the specimens were moved to a multi-purpose laboratory maintained at a constant temperature (23 ± 1) °C and relative humidity (50 ± 5)% for 360 days.

4. Strength and elastic modulus of RAC

The mean value and the corresponding coefficient of variation (COV) of the measured compressive strength and the elastic modulus are listed in Table 5. Each measurement was obtained using three identical samples. The compressive strength of the RAC was affected by the strength and service time of the parent concrete, with a maximum

Table 3
Particle size distributions and mechanical properties of aggregates.

Properties	Size of sieve (mm)	Percentage passing by weight (%)						
		NCA	RCA-S1-L	RCA-S1-M	RCA-S1-H	RCA-S20-M	RCA-S42-M	NFA
Sieve analysis	26.5	100.0	100.0	100.0	100.0	100.0	100.0	–
	19.0	67.1	67.1	67.1	67.1	66.8	66.7	–
	16.0	50.0	50.0	50.0	50.0	50.2	49.5	–
	9.5	16.7	16.7	16.7	16.7	16.8	16.7	–
	4.75	0.6	0.5	0.5	0.5	1.5	0.9	100.0
	2.36	–	–	–	–	–	–	86.2
	1.18	–	–	–	–	–	–	74.3
	0.60	–	–	–	–	–	–	52.0
	0.30	–	–	–	–	–	–	12.9
	0.15	–	–	–	–	–	–	2.4
Oven-dried density (kg/m^3)		2816	2704	2713	2708	2699	2605	2623
Surface saturation density (kg/m^3)		2827	2866	2863	2852	2842	2744	2714
Water absorption (%)		0.41	5.99	5.53	5.33	5.33	5.36	3.45
Residual mortar content (%)		–	46.3	39.4	35.8	40.1	47.9	–
Index of crushing (%)		4.3	8.7	10.9	12.4	15.2	20.2	–

Table 4
Mix proportions of natural and recycled aggregate concrete.

Notation	Mix designation	Coarse aggregate	r (%)	Mix proportions (kg/m^3)					
				Water	Cement	NFA	NCA	RCA	SP [a]
Series L:	NCA-L	100%NCA	0	180	600	610	1080	0	6.0
Low *w/c*	RCA-S42-M-50-L	50%NCA + 50% RCA-S42-M	50	180	600	603	509	509	6.0
Concrete	RCA-S42-M-100-L	100% RCA-S42-M	100	180	600	590	0	1018	6.0
	RCA-S1-L-100-L	100% RCA-S1-L	100	180	600	580	0	1030	6.0
	RCA-S1-M-100-L	100% RCA-S1-M	100	180	600	580	0	1030	6.0
	RCA-S1-H-100-L	100% RCA-S1-H	100	180	600	580	0	1030	6.0
Series M:	NCA-M	100%NCA	0	180	400	670	1180	0	4.0
Medium *w/c* Concrete	RCA-S42-M-50-M	50%NCA + 50% RCA-S42-M	50	180	400	652	551	551	4.0
	RCA-S42-M-100-M	100%RCA-P42	100	180	400	652	0	1102	4.0
	RCA-S20-M-50-M	50%NCA + 50% RCA-S20-M	50	180	400	652	564	564	4.0
	RCA-S20-M-100-M	100% RCA-S20-M	100	180	400	652	0	1129	4.0
	RCA-S1-L-100-M	100% RCA-S1-L	100	180	400	640	0	1130	4.0
	RCA-S1-M-100-M	100% RCA-S1-M	100	180	400	640	0	1130	4.0
	RCA-S1-H-100-M	100% RCA-S1-H	100	180	400	640	0	1130	4.0
Series H:	NCA-H	100%NCA	0	180	300	710	1240	0	3.0
High *w/c*	RCA-S42-M-50-H	50%NCA + 50% RCA-S42-M	50	180	300	702	593	593	3.0
Concrete	RCA-S42-M-100-H	100% RCA-S42-M	100	180	300	702	0	1185	3.0
	RCA-S1-L-100-H	100% RCA-S1-L	100	180	300	680	0	1200	3.0
	RCA-S1-M-100-H	100% RCA-S1-M	100	180	300	680	0	1200	3.0
	RCA-S1-H-100-H	100% RCA-S1-H	100	180	300	680	0	1200	3.0

[a] SP represents superplasticiser.

decrease of 19.5%. These reduction rates were consistent with those reported in our previous study [8,37]. The parent concrete strength and service time had no considerable influence on the elastic modulus of the RAC, with a maximum difference of only 8.5% and no consistent trend. This phenomenon was explained in our previous study [37].

5. Experimental results and discussions on drying shrinkage

5.1. Influence of RCA replacement ratio

The shrinkage development in each specimen over time is illustrated in Fig. 1. All specimens experienced a continuous increase in shrinkage during the test period, with a fairly rapid growth during the first few months, followed by a stabilising trend towards the end of the test period. After 112 days of drying, the shrinkage was nearly 80–93% of the final shrinkage recorded at the end of the test period (360 days), after which the shrinkage rate slowed dramatically. Therefore, it is reasonable to terminate the test after 360 days. The results predicted by the proposed model are also illustrated in Fig. 1, and are discussed in Section 6.

The relative shrinkage development in the specimens with different RCA r ratios and different parent concrete strengths (w_{or}/c_{or} ratios) is illustrated in Fig. 2. This was done by normalising the observed drying shrinkage of each specimen with its final value at the end of the test, i.e. $\varepsilon_{sh}/\varepsilon_{sh,360}$, where $\varepsilon_{sh,360}$ is the measured 360-day drying shrinkage. Fig. 2 also illustrates the predicted results using the Eurocode 2 [80] concrete model for comparison. The RCA r ratio (0%, 50%, and 100%) and w_{or}/c_{or} ratio (0.30, 0.45, and 0.60) had no observable influence on the drying shrinkage development of the RAC and the measured shrinkage variation was primarily due to the variations in the

Table 5
Mechanical properties of natural and recycled aggregate concrete.

Notation	Mix designation	C_{RM} of RCA	r (%)	f_{cm} (MPa)		E_c (GPa)		ε_{sh} (με)
				28-day	90-day	28-day	90-day	360-day
Series L:	NCA-L	–	0	57.9(2.37%)	68.2(2.2%)	39.1(3.2%)	40.4(2.5%)	411(6.8%)
Low *w/c* Concrete	RCA-S42-M-50-L	47.9%	50	58.2(0.66%)	66.9(3.7%)	34.5(1.9%)	35.7(3.7%)	492(6.5%)
	RCA-S42-M-100-L	47.9%	100	53.3(3.40%)	61.3(3.4%)	29.9(6.9%)	30.9(3.5%)	624(4.6%)
	RCA-S1-L-100-L	46.3%	100	58.2(4.85%)	66.6(4.2%)	31.7(4.8%)	32.8(2.2%)	579(4.7%)
	RCA-S1-M-100-L	39.4%	100	55.5(1.01%)	63.9(1.9%)	29.2(0.8%)	30.2(0.9%)	595(6.2%)
	RCA-S1-H-100-L	35.8%	100	53.4(1.02%)	62.1(7.3%)	31.9(0.2%)	33.0(1.2%)	656(4.5%)
Series M:	NCA-M	–	0	46.7(9.82%)	55.5(1.4%)	34.3(4.6%)	35.5(2.6%)	439(8.2%)
Medium *w/c* Concrete	RCA-S42-M-50-M	47.9%	50	44.3(1.53%)	52.5(1.8%)	31.5(3.2%)	32.6(1.8%)	490(4.5%)
	RCA-S42-M-100-M	47.9%	100	40.9(3.74%)	50.3(3.2%)	27.8(1.5%)	28.7(2.9%)	643(7.6%)
	RCA-S20-M-50-M	40.1%	50	44.7(0.76%)	52.6(1.6%)	33.0(3.2%)	34.1(4.3%)	484(4.9%)
	RCA-S20-M-100-M	40.1%	100	42.6(2.11%)	52.3(0.7%)	28.0(0.9%)	29.1(4.6%)	593(4.8%)
	RCA-S1-L-100-M	46.3%	100	46.0(0.58%)	57.6(3.2%)	27.5(3.5%)	28.4(2.2%)	584(7.2%)
	RCA-S1-M-100-M	39.4%	100	43.9(3.02%)	51.0(0.7%)	27.8(0.6%)	28.7(1.6%)	611(3.6%)
	RCA-S1-H-100-M	35.8%	100	41.1(2.29%)	50.2(5.4%)	27.4(2.8%)	28.3(2.7%)	680(4.6%)
Series H:	NCA-H	–	0	36.9(0.88%)	46.3(6.6%)	32.5(4.1%)	33.6(2.9%)	490(5.6%)
High *w/c* Concrete	RCA-S42-M-50-H	47.9%	50	32.1(6.62%)	38.3(0.7%)	30.4(4.4%)	31.4(3.3%)	508(7.4%)
	RCA-S42-M-100-H	47.9%	100	28.4(3.97%)	34.6(3.0%)	27.2(2.2%)	28.1(2.1%)	625(6.3%)
	RCA-S1-L-100-H	46.3%	100	33.1(1.53%)	43.0(3.4%)	27.1(3.0%)	28.0(0.5%)	628(4.9%)
	RCA-S1-M-100-H	39.4%	100	32.4(6.16%)	40.1(4.3%)	27.1(2.0%)	28.0(6.2%)	650(6.6%)
	RCA-S1-H-100-H	35.8%	100	31.6(1.67%)	39.6(2.2%)	27.7(6.8%)	28.6(3.5%)	710(7.2%)

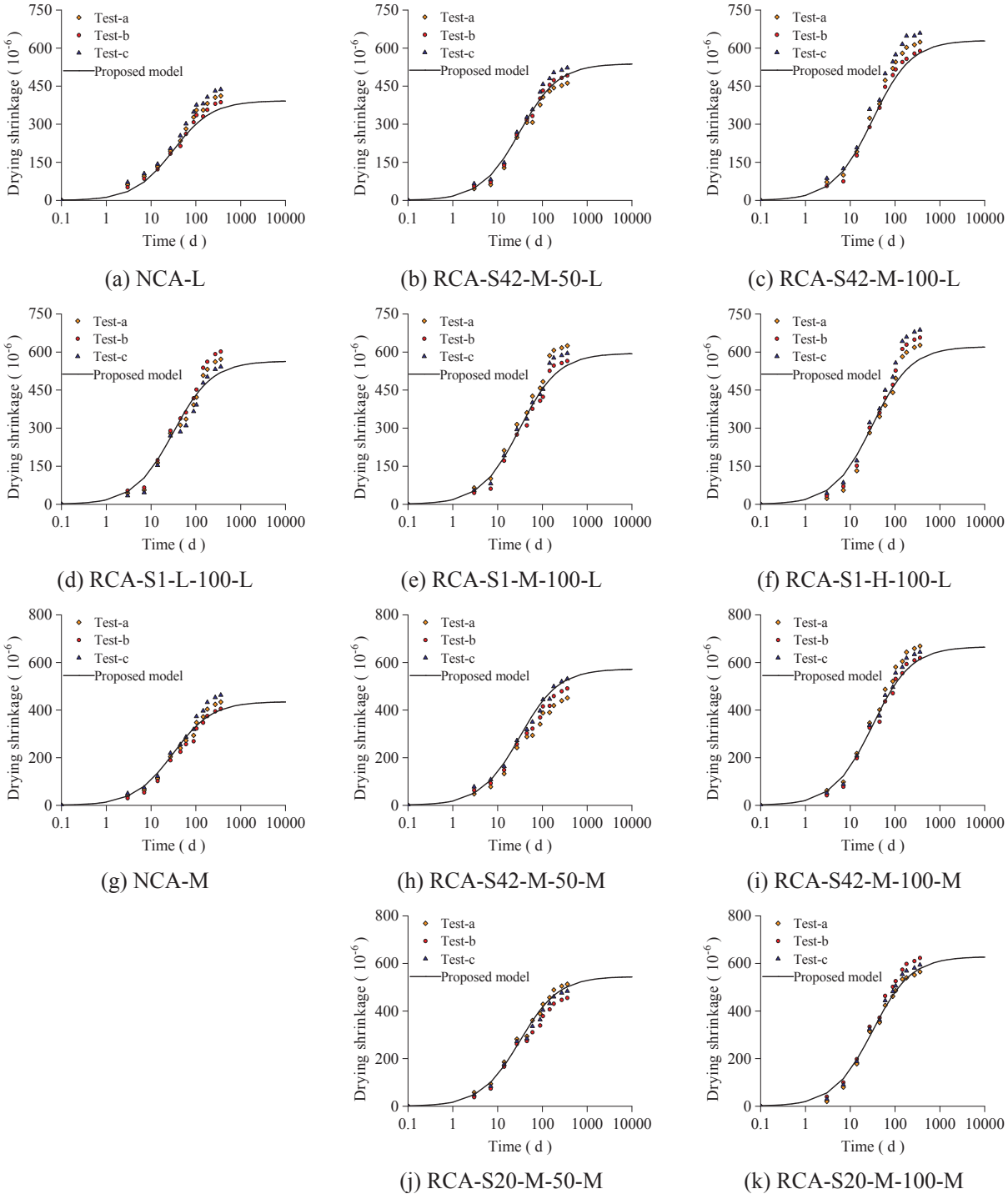

Fig. 1. Measured drying shrinkage of concrete with different types of RCA.

environmental conditions. Additionally, the expressions provided in Eurocode 2 described the shrinkage development of the concrete specimens reasonably well, with a maximum error of 15%. Thus, the impact of the quality of parent concrete on the drying shrinkage of RAC can be investigated using the shrinkage amplification factor (κ_{sh}) i.e. the ratio of the drying shrinkage of the RAC to that of the reference NAC.

As illustrated in Fig. 3, the drying shrinkage of all samples increased with the increase in RCA *r* ratio, regardless of the other test variables. Compared to the reference NAC, the RAC specimens experienced increases of 3.6–19.7% and 27.6–59.6% in their 360-day drying shrinkage values for RCA *r* ratios of 50% and 100%, respectively. These increases conform to those reported in other studies [61]. Furthermore, as expected, smaller compressive strengths (larger *w/c* ratios) lead to larger drying shrinkage in the NAC. For example, the NAC with a compressive strength of 36.9 MPa (*w/c* = 0.60) had a 19.2% larger drying shrinkage than that with a compressive strength of 57.9 MPa (*w/c* = 0.30) (Fig. 3(a)). Smaller differences were obtained for the RAC. For example, in the concrete with 100% RCA-S42-M (Fig. 3(a)), a limited increment of 3% was observed as the *w/c* ratio decreased to 0.30 from 0.60.

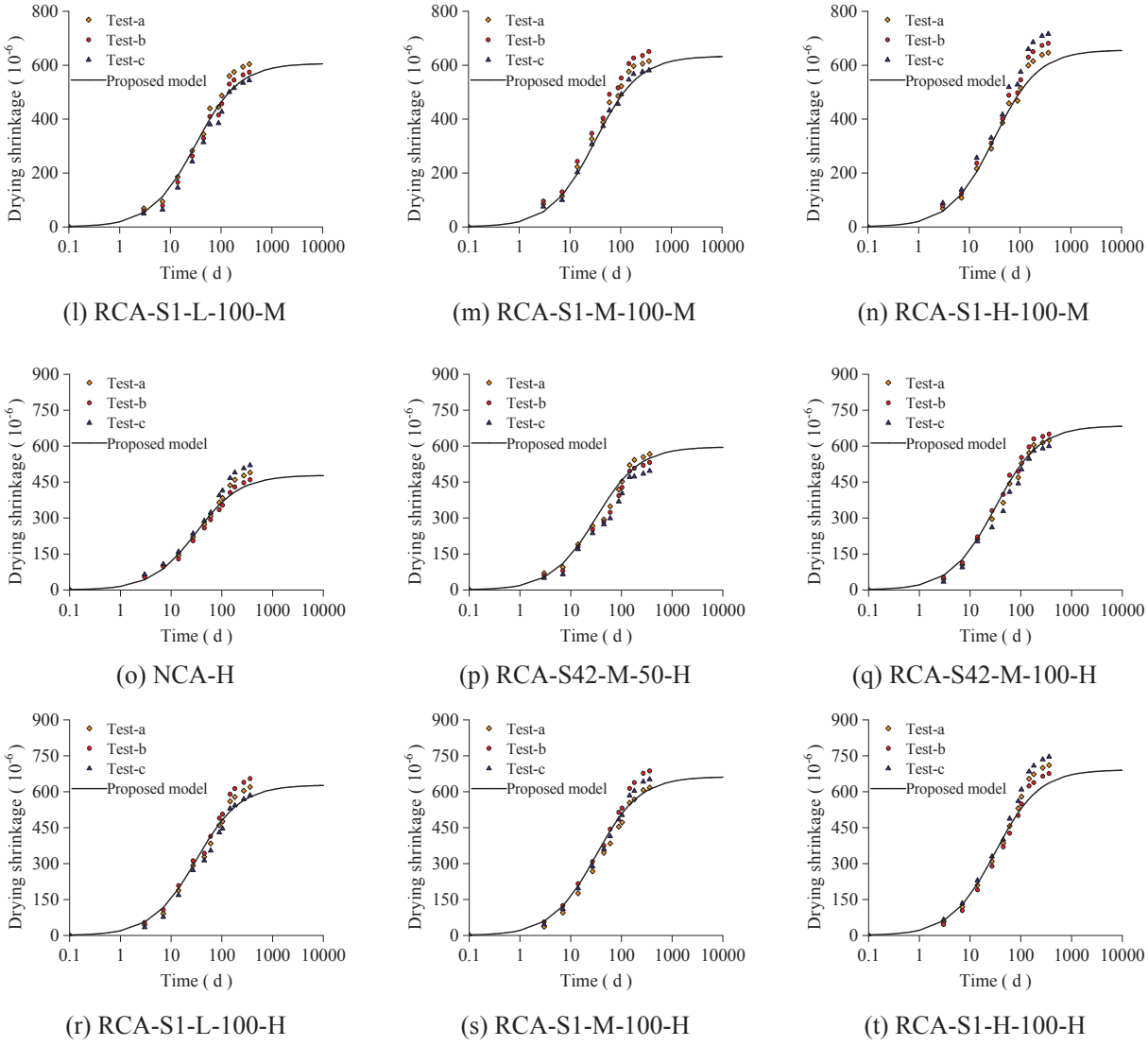

Fig. 1. (*continued*)

5.2. Influence of service time of parent concrete

The impact of the service time of the parent concrete on the drying shrinkage of RAC is quite limited. Fig. 4 compares the 360-day drying shrinkage of the RAC with 100% RCAs from parent concrete of different service times. The drying shrinkage of the RAC clearly exhibits similar values. For example, in the low w/c concrete (Series L), the measured 360-day drying shrinkage of the RCA-S1-M-100-L specimen with 1-year-old RCA and the RCA-S42-M-100-L specimen with 42-year-old RCA was 595 με and 624 με, respectively, with a difference of 4.6% and the concrete with the older RCAs experiencing a larger drying shrinkage. Similar observations were made for medium w/c concrete (Series M) and high w/c concrete (Series H), with maximum differences of 8.4% and 3.8%, respectively.

5.3. Influence of strength of parent concrete

Fig. 5 illustrates the influence of the strength of parent concrete on the drying shrinkage of RAC. RCAs from parent concrete with higher strength (lower w_{or}/c_{or}) led to lesser shrinkage in the RAC, even though RCAs from higher strength parent concrete have larger C_{RM} values than those from lower strength parent concrete (larger C_{RM} values generally result in a larger shrinkage in RAC). In particular, in Series L (w/c = 0.30), the RAC shrinkage using RCA-S1-H (C_{RM} = 35.8%) was 59.6% higher than that of the reference NAC-L, while the shrinkage increase percentage decreased to 44.8% when using RCA-S1-M (C_{RM} = 39.4%) and to 40.9% when using RCA-S1-L (C_{RM} = 46.3%). For the RAC with w/c = 0.45, the shrinkage increase percentage decreased from 54.9% for RCA-S1-L to 39.2% and 33.0% for RCA-S1-M and RCA-S1-H, respectively. For the RAC with w/c = 0.60, the shrinkage increase percentage decreased from 44.9% for RCA-S1-L to 32.6% and 28.2% for RCA-S1-M and RCA-S1-H, respectively. This probably happens because the RCAs from parent concrete with a lower w_{or}/c_{or} have a lower porosity and a more uniformly hardened cement paste which increases the shrinkage deformation of the RAC. The large influence of parent concrete strengths on drying shrinkage clearly highlights why residual mortar content cannot serve as the only parameter required to evaluate the shrinkage amplification factor of RAC.

A similar investigation was also conducted by Kou and Poon (2015) [25] and Gholampour and Ozbakkalogu (2018) [65]. Fig. 6(a) illustrates the measured shrinkage amplification factor of the RAC specimens using RCAs from parent concrete of 30–100 MPa, as investigated by Kou and Poon [25]. The higher-strength parent concrete clearly led to a smaller shrinkage amplification factor for water-to-binder (w/b) ratios of both 0.35 and 0.50. Particularly, the concrete with r = 100% had a shrinkage amplification factor of 1.246–1.354 when using 30 MPa parent concrete, which decreased to 1.042–1.157 when using 100 MPa parent concrete. This phenomenon is even more significant in high-

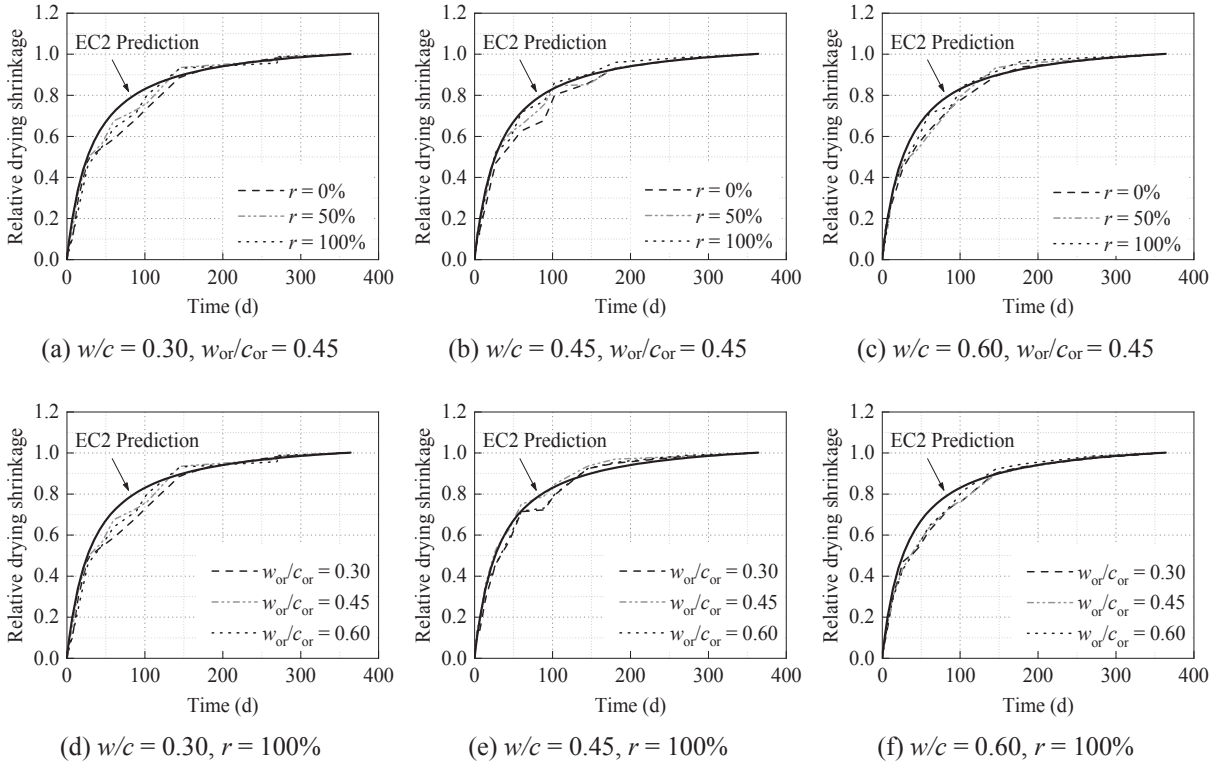

Fig. 2. Relative shrinkage development over time.

strength RAC [65]. In the RAC specimens with a target compressive strength of 80 MPa, the shrinkage increase after 360 days was nearly 100% when using 20 MPa parent concrete, but reduced significantly to about 7% when using parent concrete with a strength of 110 MPa. Although the RCAs from the 20 MPa and 110 MPa parent concrete had similar residual mortar contents of 42–53%, the difference in their shrinkage amplification factors was nearly 100%. This further substantiates the need to account for the parent concrete strength in the

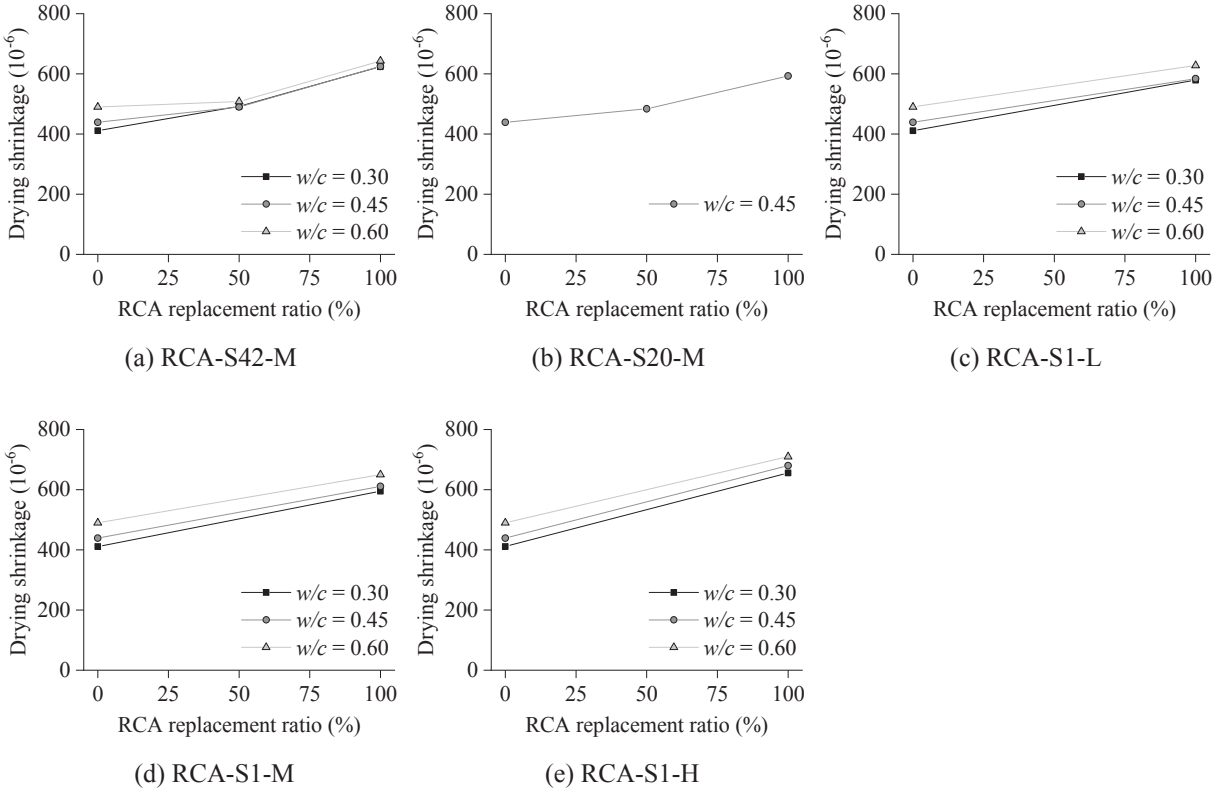

Fig. 3. Influence of RCA *r* ratios on the drying shrinkage.

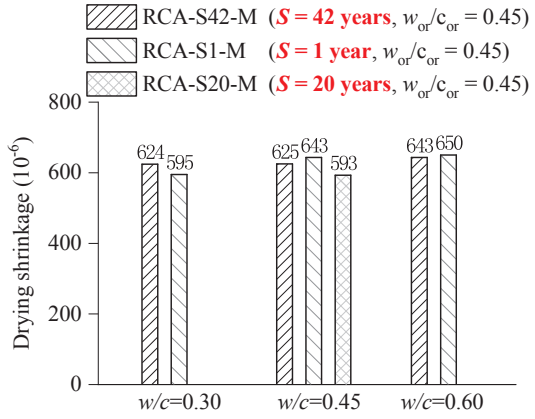

Fig. 4. Influence of service time of parent concrete on the drying shrinkage of RAC (r = 100%).

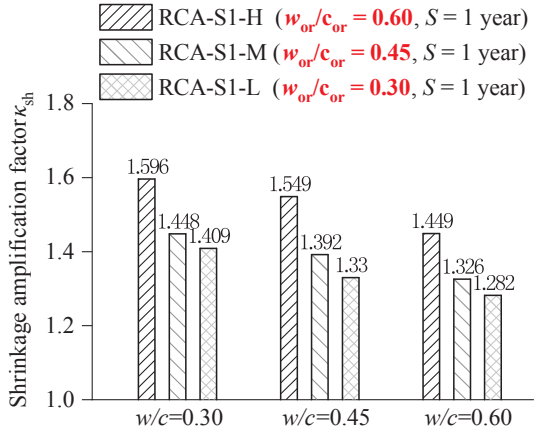

Fig. 5. Influence of parent concrete strength on the drying shrinkage of RAC using the shrinkage amplification factor κ_{sh}.

prediction model, in addition to residual mortar content.

Gonzalez-Corominas and Etxeberria also observed similar tendencies. When RCAs from 60 to 100 MPa parent concrete were used to prepare 100 MPa RAC, shrinkage amplification factors of 1.55–1.38 were obtained. However, this value increased significantly to 2.13 when using RCAs from 40 MPa parent concrete [59] (Fig. 7). Fig. 7 also illustrates that the linear correlation between the shrinkage amplification factor and the physical properties of the aggregate (density and water absorption of the aggregate) no longer exists due to the use of aggregates from parent concrete with different strengths.

Pedro et al. (2014) [66] prepared three groups of RAC using RCA r = 100% and parent concrete with strengths equivalent to that of the RAC, i.e. 20 MPa, 45 MPa, and 65 MPa. Similar shrinkage amplification factors were observed for all three groups of the RAC. As similar compressive strength values were selected for both the parent concrete and the RAC, the properties of the residual mortar in the RCA and that of the fresh mortar in the RAC were similar, and accordingly, similar shrinkage factors were obtained.

The above-mentioned experiments suggest that similar shrinkage amplification factors are observed when the properties of the parent concrete and the RAC are similar, and varied shrinkage amplification factors are observed when the properties of the parent concrete and the RAC are different, i.e. a larger shrinkage amplification factor for a lower-strength parent concrete and vice versa. Furthermore, this impact cannot be effectively represented by the r ratio, C_{RM}, or physical properties of the RCAs. Therefore, an additional parameter is required to describe the shrinkage difference between RAC and NAC–the strength of parent concrete.

6. Modified drying shrinkage model for RAC

This study aims to propose a new model to estimate the shrinkage amplification factor κ_{sh}, in which the strength of parent concrete is further accounted in addition to the residual mortar content (C_{RM}). To predict the drying shrinkage of RAC, the proposed κ_{sh} can be combined with the existing shrinkage models for NAC. Here, the EC 2 model [80] was selected to combine the proposed κ_{sh}, as it predicted the time-dependent relative shrinkage of both NAC and RAC reasonably well, as illustrated in Fig. 2.

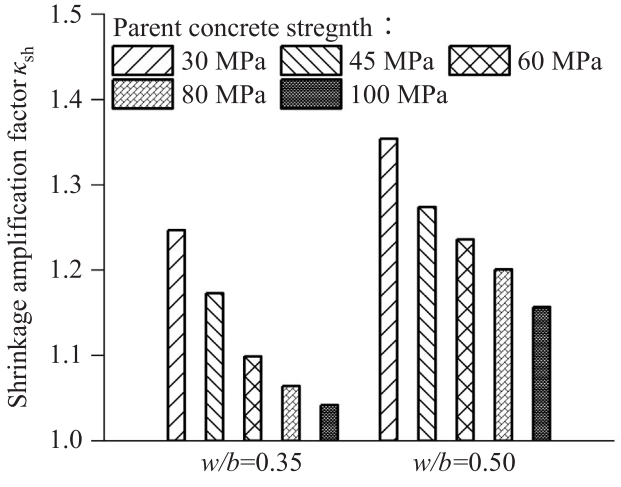

(a) Slight variation in κ_{sh} with RCAs from 30–100 MPa parent concrete as investigated by Kou and Poon [25]

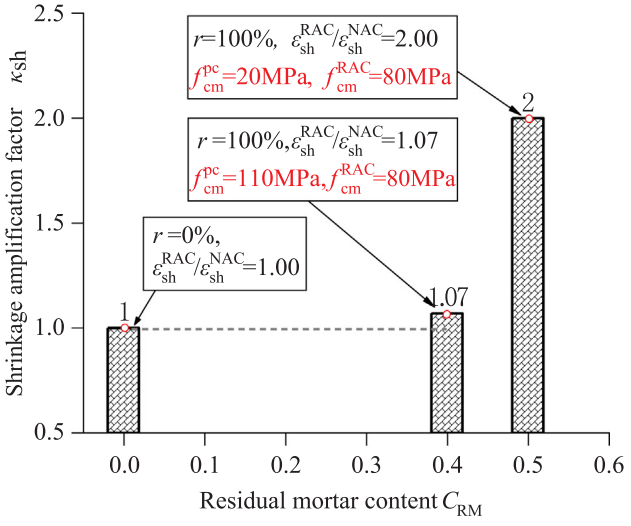

(b) Significant variation in κ_{sh} with RCAs from 110 MPa parent concrete and 20 MPa parent concrete as investigated by Gholampour and Ozbakkalogu [65]

Fig. 6. Reduction in the shrinkage amplification factor κ_{sh} when using higher-strength parent concrete.

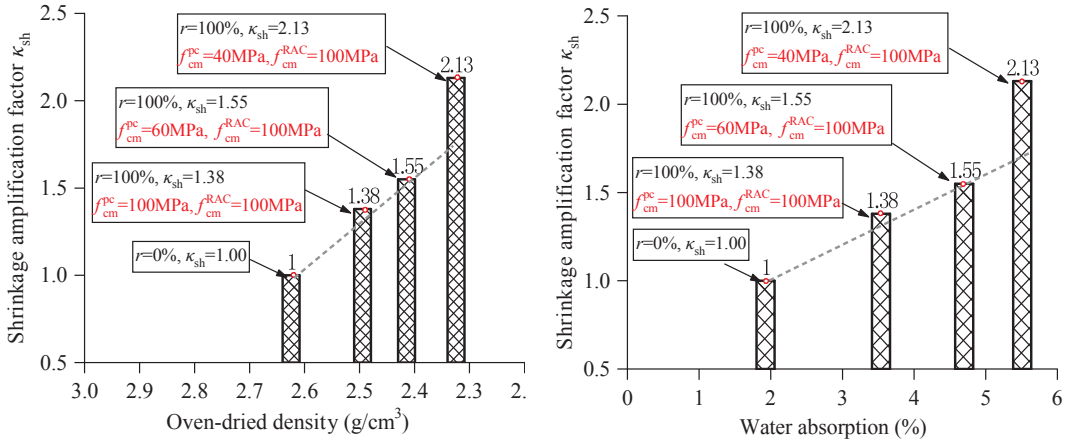

(a) Nonlinear variation between κ_{sh} and aggregate density

(b) Nonlinear variation between κ_{sh} and aggregate water absorption

Fig. 7. Significant variation in κ_{sh} with decreasing parent concrete strength as investigated by Gonzalez-Corominas and Etxeberria [59], (a) Nonlinear variation between κ_{sh} and aggregate density, (b) Nonlinear variation between κ_{sh} and aggregate water absorption.

6.1. Modified drying shrinkage model

Concrete is generally considered to be a two-phase composite material (consisting of mortar and coarse aggregate) [45]. Drying shrinkage is caused by the evaporation of water from mortar and is restricted by the presence of coarse aggregates. Therefore, Eq. (1) can be used to calculate the drying shrinkage of NAC, where ε_{sh}^{NAC} represents the NAC shrinkage strain, while ε_{sh}^{NM} stands for the shrinkage strain of the new mortar, V_{NCA}^{NAC} is the volumetric content of NCA in the NAC, and n is a constant that is related to the stiffness of the NCA, with a value that ranges between 1.2 and 1.7.

$$\varepsilon_{sh}^{NAC} = \varepsilon_{sh}^{NM}\cdot(1 - V_{NCA}^{NAC})^n \tag{1}$$

RCA can also be treated as a two-phase composite material consisting of the original virgin aggregate (OVA) and residual mortar (RM), and hence the shrinkage strain of RAC can be obtained as shown in Eq. (2).

$$\varepsilon_{sh}^{RAC} = \varepsilon_{sh}^{TM}\cdot(1 - V_{TNCA}^{RAC})^n \tag{2}$$

Here, ε_{sh}^{RAC} is the drying shrinkage strain of the RAC and ε_{sh}^{TM} represents the drying shrinkage strain of the new and residual mortar. V_{TNCA}^{RAC} is the total volumetric content of the stone particles in the RAC, which can be estimated using Eq. (3).

$$V_{TNCA}^{RAC} = V_{NCA}^{RAC} + V_{OVA}^{RAC} = (1 - r\cdot CRM)\cdot V_{CA}^{RAC} \tag{3}$$

where V_{OVA}^{RAC} is the volumetric content of the OVA in the RAC and V_{CA}^{RAC} is the volumetric content of the coarse aggregate (CA) in the RAC.

Generally, the shrinkage performance of the cement paste of RAC is similar to that of NAC, and the volumetric content of NCA in NAC (V_{NCA}^{NAC}) is equal to the total volumetric content of coarse aggregate (V_{CA}^{RAC}, including both NCA and RCA). Considering the relationship between V_{NCA}^{NAC} and V_{CA}^{RAC}, the shrinkage strain of RAC can be estimated by combining Eqs. (1)–(3), to obtain Eq. (4). Furthermore, the constant factor n was set to 1.45, which is the mean of the empirical values of 1.2–1.7.

$$\kappa_{sh} = \frac{\varepsilon_{sh}^{RAC}}{\varepsilon_{sh}^{NAC}} = \frac{\varepsilon_{sh}^{TM}}{\varepsilon_{sh}^{NM}}\cdot\left(\frac{1 - (1 - r\cdot CRM)\cdot V_{CA}^{RAC}}{1 - V_{CA}^{RAC}}\right)^n \tag{4}$$

To ease understanding this equation, the shrinkage amplification factor κ_{sh} can be expressed as the product of $\kappa_{sh,f}$ and $\kappa_{sh,a}$, as shown in Eq. (5).

$$\kappa_{sh} = \kappa_{sh,f}\cdot\kappa_{sh,a} \tag{5}$$

where $\kappa_{sh,f}$ represents the difference in the drying shrinkage between the total mortar (natural mortar and residual mortar) in RAC and natural mortar in NAC, as shown in Eq. (6).

$$\kappa_{sh,f} = \varepsilon_{sh}^{TM}/\varepsilon_{sh}^{NM} \tag{6}$$

while $\kappa_{sh,a}$ represents the reduction in the capacity of restriction to the drying shrinkage of natural mortar, which is caused by the volume change of the stone particles in RAC.

$$\kappa_{sh,a} = \left(\frac{1 - (1 - r\cdot CRM)\cdot V_{CA}^{RAC}}{1 - V_{CA}^{RAC}}\right)^n \tag{7}$$

Considering that concrete with higher compressive strength causes lower shrinkage in the corresponding mortar and vice versa, the shrinkage of mortar is influenced by the compressive strength of the concrete according to EC2 model [80]. Thus, the drying shrinkage of natural mortar is related to the strength of the concrete, as shown in Eq. (8), wherein, $f(R_H)$ is a function of the ambient relative humidity (R_H), f_{cm}^{NAC} is the compressive strength of NAC, exp() refers to $e^{()}$, and a is a coefficient that reflects the correlation between the mortar shrinkage and the compressive strength of concrete.

$$\varepsilon_{sh}^{NM} = f(R_H)\cdot\exp(a\cdot f_{cm}^{NAC}) \tag{8}$$

Similarly, the shrinkage of the total mortar (new mortar and residual mortar) can be calculated using Eq. (9).

$$\varepsilon_{sh}^{TM} = f(R_H)\cdot\left[\frac{V_{NM}^{RAC}}{V_{TM}^{RAC}}\cdot\exp(a\cdot f_{cm}^{NAC}) + \frac{V_{RM}^{RAC}}{V_{TM}^{RAC}}\cdot\exp(b\cdot f_{cm}^{PC})\right] \tag{9}$$

where V_{RM}^{RAC}, V_{NM}^{RAC}, and V_{TM}^{RAC} are the volume fractions of the residual mortar, natural mortar, and total mortar in RAC, respectively, f_{cm}^{PC} and f_{cm}^{NAC} are the compressive strengths of the parent concrete and NAC, respectively, and b is a coefficient that reflects the correlation between the drying shrinkage of residual mortar and the compressive strength of the parent concrete.

Thus, $\kappa_{sh,f}$ in Eq. (6) is rewritten as Eq. (10) to quantify the influence of the residual mortar quality on the drying shrinkage of RAC.

$$\kappa_{sh,f} = \frac{\frac{V_{NM}^{RAC}}{V_{TM}^{RAC}}\cdot\exp(a\cdot f_{cm}^{NAC}) + \frac{V_{RM}^{RAC}}{V_{TM}^{RAC}}\cdot\exp(b\cdot f_{cm}^{PC})}{\exp(a\cdot f_{cm}^{NAC})} \tag{10}$$

To predict the drying shrinkage of RAC, its compressive strength is preferred over that of NAC, in which case, $\exp(a\cdot f_{cm}^{NAC})$ can be replaced by $\exp(c\cdot f_{cm}^{RAC})$, and Eq. (10) can be rewritten as Eq. (11).

$$\kappa_{sh,f} = \frac{\frac{V_{NM}^{RAC}}{V_{TM}^{RAC}} \cdot \exp(c \cdot f_{cm}^{RAC}) + \frac{V_{RM}^{RAC}}{V_{TM}^{RAC}} \cdot \exp(b \cdot f_{cm}^{PC})}{\exp(c \cdot f_{cm}^{RAC})} \quad (11)$$

where c is the coefficient that reflects the correlation between the shrinkage of natural mortar in RAC and the RAC compressive strength. Accurately estimating the values of b and c in Eq. (11) is of great importance. A drying capacity of 70% can be observed in old concrete when it is placed in water (or in an environment with higher humidity) [81], which is similar to the process used to prepare RCAs under saturated-surface-dry (SSD) condition. Therefore, $\exp(b \cdot f_{cm}^{PC})$ can be estimated to be 70% of $\exp(c \cdot f_{cm}^{RAC})$. Using the 1stOpt software, the coefficients b and c were regressed to -0.040 and -0.045, respectively, based on the 20 groups of measurements performed in this study. It is worth noting that the proposed model is almost entirely theoretical, with only two regressed coefficients. Therefore, it should provide a higher accuracy across a wider range of parameter values than the existing models that are directly regressed based on a limited database.

6.2. Validation of the proposed drying shrinkage model

Eqs. (7) and (11) were combined with the EC2 model to predict the drying shrinkage of RAC, and the proposed model was benchmarked against the measured drying shrinkage of the RAC specimens from this study and others [21,25,26,36,54,59,60,65,66]. Detailed information of these tests is listed in Table 6. In particular, the material properties included the compressive strengths of the parent concrete that range from 20 MPa to 110 MPa, and the crushing age that ranges from 2 months to 42 years. RCA r ratios of 0–100% were used to prepare the RAC with compressive strengths of 20–104 MPa. The relative humidity during the test ranged from 40% to 77% over a duration of 54–448 days.

Fig. 1 compares the measured and predicted drying shrinkage using the proposed model. As illustrated in Fig. 1(a), (g), and (o), a maximum underestimation of 20% was obtained for the reference NAC with different w/c ratios of 0.30, 0.45, and 0.60, during the test period. This variation is quite acceptable, as a difference of almost 30–40% between the measured and predicted shrinkage values occurs due to the combined effect of the variations in the experiment [81]. Similarly, the proposed model slightly underestimated the drying shrinkage of the RAC, as illustrated in Fig. 1(b)–(f) for a w/c ratio of 0.30, Fig. 1(h)–(n) for a w/c ratio of 0.45, and Fig. 1(p)–(t) for a w/c ratio of 0.60. As the aim of this study is to propose an RAC drying shrinkage model with a similar degree of accuracy to that of NAC, a comparison between the measured and calculated κ_{sh}, using the proposed model, is illustrated in Fig. 8. To highlight the influence of parent concrete strength on the drying shrinkage of RAC, the predicted results without the influence of parent concrete strength ($\kappa_{sh,f} = 1.0$) are also illustrated in Fig. 8. Notably, for all three concrete mixtures, the proposed model can predict κ_{sh} of RAC reasonably well, however, a different trend could be captured by ignoring the influence of the parent concrete strength.

A comparison between the predicted κ_{sh} values at the end of the experiment, and the measured κ_{sh} values of the RAC specimens from this study and others, a total of 95 groups of results from 262 samples, is illustrated in Fig. 9. While several more drying shrinkage measurements could have been obtained from similar literature, they are not included in this study due to a lack of details regarding the parent concrete strength. For comparison, the predicted results using RAC drying shrinkage models available in similar literature are also illustrated in Fig. 9, including models considering the residual mortar content [45], weighted aggregate density [62,63], and weighted aggregate water absorption [62,63]. Fig. 9(a) illustrates that the modified shrinkage model proposed herein matches with the RAC κ_{sh} reasonably well, exhibiting the closest mean value and the smallest coefficient of variation (COV). The mean value of the predicted and experimental κ_{sh} values was 0.992, and the corresponding COV was 9.10%. The other models

Table 6
Material properties and experimental conditions for the tested RAC.

Authors	Information of Parent concrete			R (%)	RCA Moisture	f_{cm} (MPa)	E_c (GPa)	Shrinkage test parameter and results					
	f_{cm} (MPa)	S (year)	Crushing method [a]					Test conditions	t_s [b] (d)	t-t_s [c] (d)	Sample type and size (mm)	No. of samples	ε_{sh} (με)
Ajdukiewicz and Kliszczewicz (2002) [36]	63.2/72.3	3–7	N/A	0/100	SSD	50–54	30–40	N/A	N/A	360	Prism: 100 × 100 × 500	24 samples (4 groups)	550–690
Manzi et al. (2013) [21]	36	15	T2	0/51.9	Wet condition	41/51	30/31	20 °C, 60%	2	448	Cylinder: Φ120 × 240	6 samples (2 groups)	431–771
Pedro et al. (2014) [66]	21–65.7	N/A	T1 + T2	0–100	SSD	20–72	25–48	20 °C, 60%	N/A	91	Prism: 150 × 150 × 600	36 samples (18 groups)	300–500
Kou and Poon (2015) [25]	30–100	N/A	N/A	0/100	SSD	45–65	32–38	23 °C, 50%	3	112	Prism: 75 × 75 × 285	36 samples (12 groups)	480–700
Gonzalez-Corominas and Etxeberria (2016) [59]	40–100	1/2–3	N/A	0–100	SSD	90–104	37–50	23 °C, 50%	3	360	Prism: 75 × 75 × 285	30 samples (10 groups)	310–775
Gholampour and Ozbakkaloglu (2018) [65]	20–110	1/6	N/A	0–100	SSD	40–80	30–41	23 °C, 50%	N/A	448	Prism: 75 × 75 × 285	18 samples (6 groups)	418–814
Gomez-Soberon (2003) [54]	30.7	N/A	TI	0–100	Wet condition	28–30	27–30	20 °C, 50%	28	90	Cylinder: Φ150 × 450	10 samples (5 groups)	374–403
Ravindrarajah and Tam (1985) [26]	23–34	N/A	TI	0/100	SSD	19–34	30–42	30 °C, 77%	28	70	Prism: 100 × 100 × 400	24 samples (12 groups)	255–497
Yang and Lim (2018) [60]	35.6	N/A	TI	0–68	SSD	42–47	25–28	20 °C, 40%	N/A	54	Prism: 100 × 100 × 400	18 samples (6 groups)	858–993
This study	36.9–62.7	1–42	T2	0–100	SSD	28–58	27–39	23 °C, 50%	28	360	Prism: 100 × 100 × 400	60 samples (20 groups)	411–710
Total number of specimens												262 samples (95 groups)	

[a] T1 represents the crushing method using an impact crusher; T2 is obtained using an impact crusher and a hammer mill.
[b] t_s is the beginning day of drying shrinkage.
[c] $t - t_s$ is the drying time of test samples.

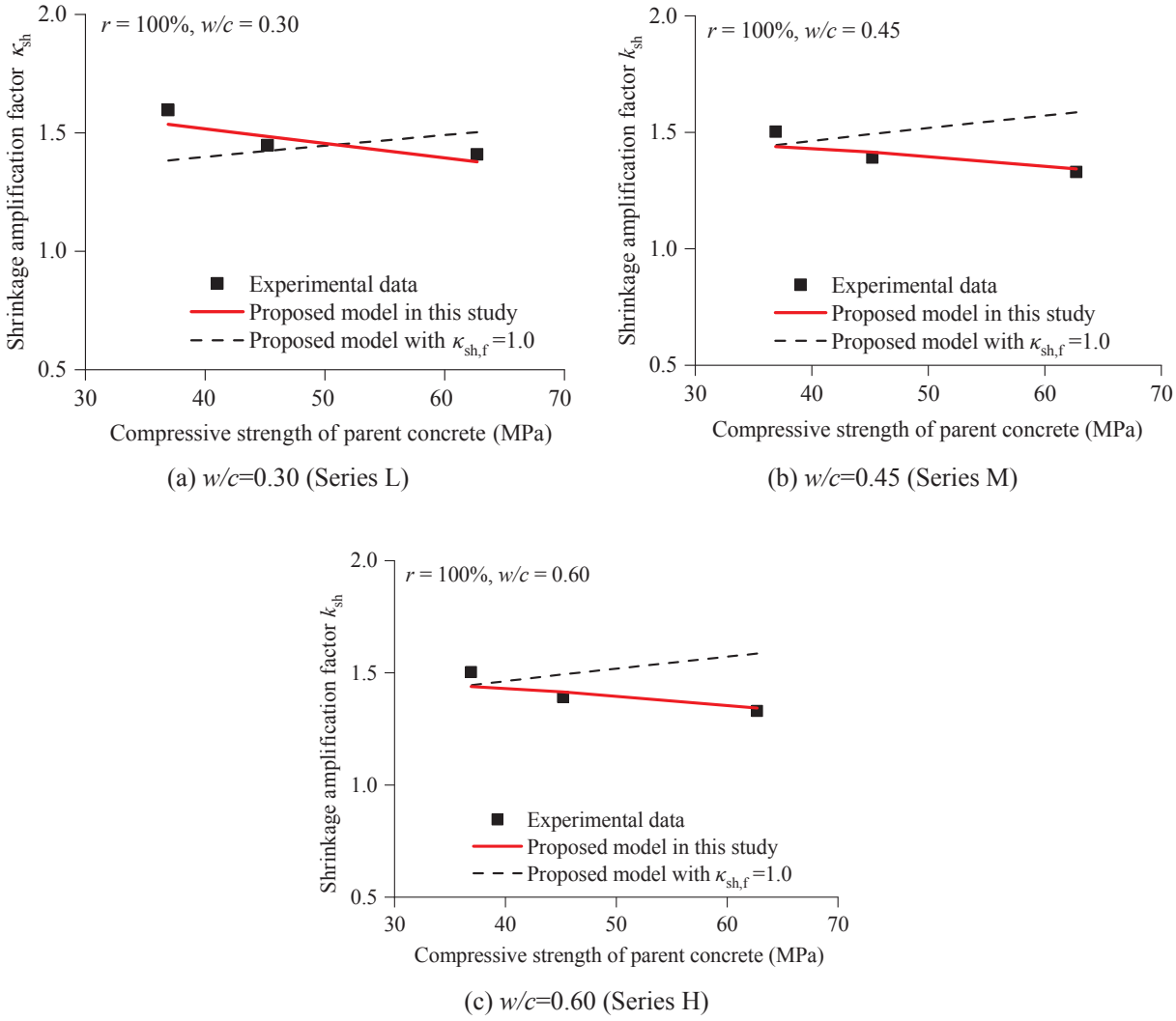

Fig. 8. Comparison between the experimental and predicted κ_{sh} for different parent concrete strengths.

generated mean values of 0.908–0.969, and COVs between 16.92% and 19.60% (Fig. 9(b)–(d)).

Furthermore, the error between the calculated and measured κ_{sh} values are almost entirely within a range of ± 15% for the proposed model (Fig. 9(a)), while the shrinkage models that do not consider the parent concrete strength significantly overestimated or underestimated the shrinkage of RAC, particularly when the difference between the RAC strength and parent concrete strength is reasonably large. For example, as illustrated in Fig. 9(b), the model only considering the influence of C_{RM} overestimated the shrinkage amplification factor by 33.5–35.1% for the 40–80 MPa RAC prepared using 110 MPa parent concrete [65], and significantly underestimated the shrinkage amplification factor by up to 67.2% for the 100 MPa RAC prepared using RCAs from lower-strength parent concrete [59].

6.3. Parametric study

To identify the quality of newly proposed model, a parametric study was conducted. The considered parameters included compressive strength of parent concrete and recycled concrete in the range of 20–80 MPa, RCA r ratio of 0–100%, C_{RM} of RCA between 20% and 60%. The drying shrinkage were estimated under the relative humidity of 30–80% for 50 years.

Fig. 10 illustrates the influence of r ratios on the drying shrinkage of RAC when using RCAs with different C_{RM} values. Identical strengths of 20–80 MPa were specified for both the RAC and the parent concrete. For RCA r = 100%, with a C_{RM} of 20%, the drying shrinkage of the RAC with strengths of 20 MPa, 50 MPa, and 80 MPa increased by 17.4%, 20.2%, and 20.7%, respectively, compared to that of the NAC. These percentages significantly increased with the increase in C_{RM} values. For example, when using RCAs with a C_{RM} of 60%, the increase in drying shrinkage of the corresponding RAC specimens were 55.2%, 64.0%, and 64.8%, respectively. These increments are consistent with those reported previously [20]. Notably, when identical compressive strengths were specified for both the RAC and the parent concrete, as illustrated in Fig. 10, the shrinkage increases in the RAC were similar, with a maximum error of 2.8% and 6.1%, for C_{RM} values of 20% and 60%, respectively. This phenomenon is also consistent with previous studies [66].

Fig. 11 describes the changes in the drying shrinkage of RAC when using RCAs with varying parent concrete strengths and the drying shrinkage of RAC specimens with strengths of 30 MPa and 60 MPa, and RCA r ratios of 0%, 25%, 50%, 75%, and 100% are illustrated. The utilisation of higher strength parent concrete clearly helps reduce the drying shrinkage of RAC, regardless of the strength of the RAC. When using RCA r = 100% from 30 MPa parent concrete, drying shrinkage increases of 20.1% and 67.0% were observed in the RAC with strengths of 30 MPa and 60 MPa, respectively, compared to that of the NAC. This significantly decreased to 9.3% and 12.5%, respectively, when using RCAs from 80 MPa parent concrete. This trend coincides with the

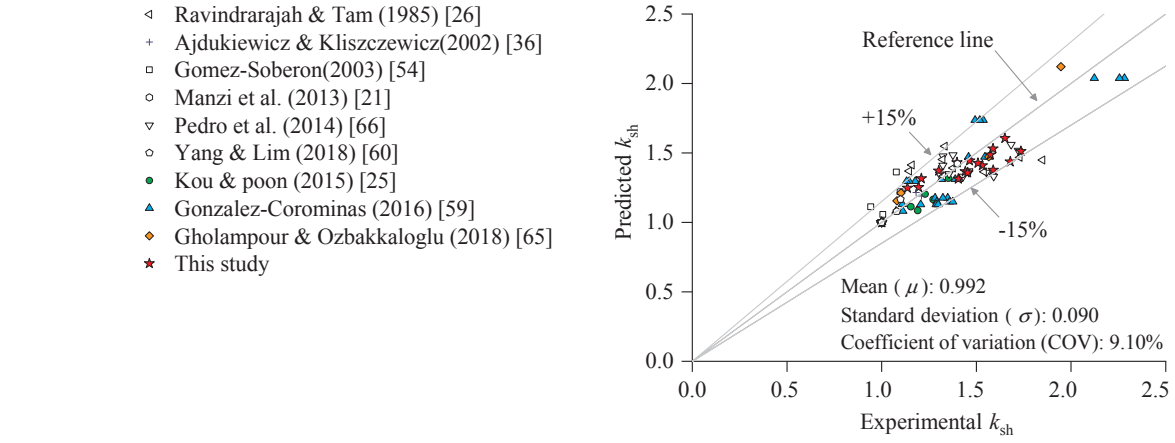

(a) Model proposed in this study

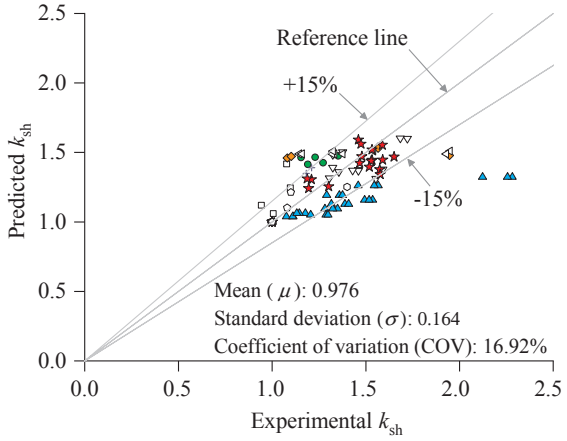

(b) Model including residual mortar content

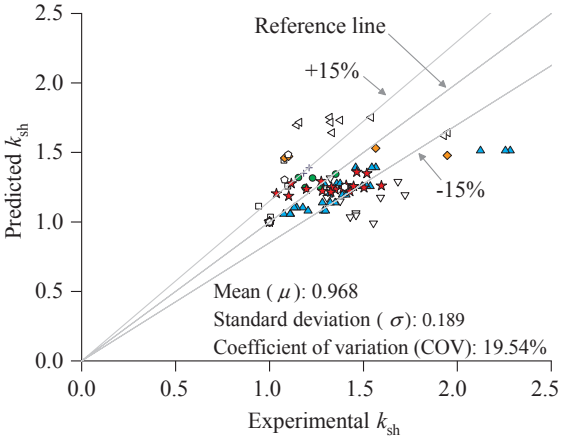

(c) Model including weighted density of aggregates

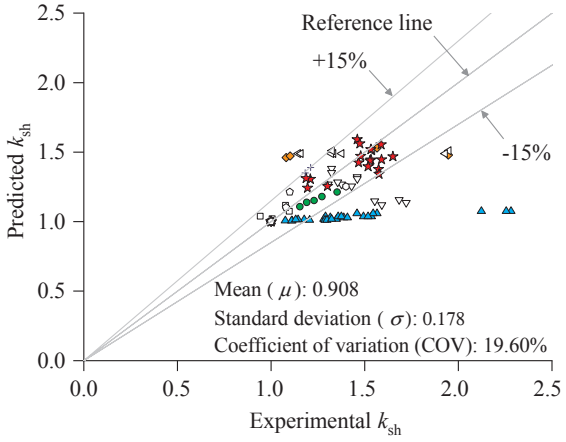

(d) Model including weighted water absorption of aggregates

Fig. 9. Comparison between the predicted and measured κ_{sh} using different models.

findings reported previously in Section 5.

Fig. 12 illustrates the effect of relative humidity on the drying shrinkage of NAC and RAC, with identical strengths specified for the RAC and the parent concrete. The drying shrinkage decreased with the increase in relative humidity, and identical decreases of 34.5% were obtained for both NAC and RAC. This is primarily because, according to EC2 model (shown in Appendix A), the effects of relative humidity and compressive strength on the drying shrinkage of concrete are separate.

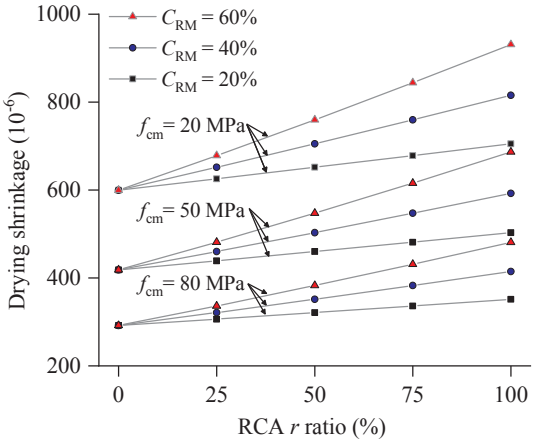

Fig. 10. Parametric study: influence of RCA *r* ratio on the drying shrinkage of RAC.

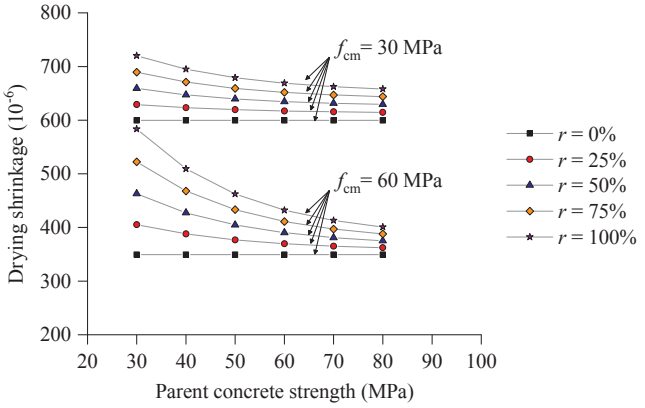

Fig. 11. Parametric study: influence of parent concrete on the drying shrinkage of RAC.

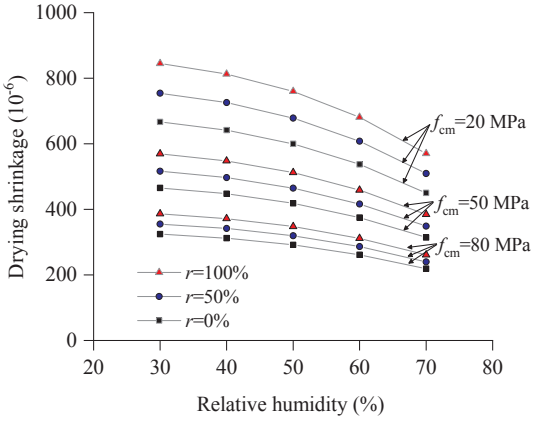

Fig. 12. Parametric study: influence of relative humidity on the drying shrinkage of RAC.

Further experimental effort to evaluate the influence of relative humidity on the drying shrinkage of concrete is required to properly benchmark the proposed model.

The above comparative results showed that the proposed model could provide reasonable predictions in the drying shrinkage for RAC with a relatively wide range of parameters, as it was theoretically developed based on the shrinkage mechanism and was capable of reflecting the characteristics of RCAs. Despite of this, further investigation may still be required to simplify this refined model and finally include the simplified one in the designing code. For the simplification, the parameters in this refined model, e.g. the volume of coarse aggregate in concrete, the residual mortar content, and the parent concrete strength, etc., could be replaced with the ones that are more applicable in structural design, e.g. the concrete mix, the bulk density of the coarse aggregate, and the compressive strength of the resulting concrete, etc. For instance, with proper research procedures, the aggregate-to-cement mass ratio can be used to replace the coarse aggregate volume in the newly model; and the RCA density can be used to reflect the combined effect of the residual mortar content and parent concrete strength on the shrinkage behaviour. Similar research procedures could be found in research papers on lightweight aggregate concrete.

7. Conclusions

This study aims at investing the effects of parent concrete on the drying shrinkage of RAC, and theoretically proposing a drying shrinkage model for RAC to account for these influences. Hence, RAC was prepared with three groups of RCAs from the laboratory and two groups of RCAs from real demolished projects. The compressive strength of the parent concrete was controlled by water-to-cement ratios of 0.30, 0.45, and 0.60; meanwhile, the service time of the parent concrete ranged from 20–42 years to 1 year. The water-to-cement ratios of 0.30, 0.45, and 0.60, and the RCA replacement ratios of 0%, 50%, and 100% were assessed for the RAC. The drying shrinkage test was conducted for 360 days. Using the test data obtained from this test, a new drying shrinkage model was theoretically derived and benchmarked against available experimental data collected from this study and from the literature.

Similar shrinkage amplification factors κ_{sh} were observed when the properties of the parent concrete and the RAC were similar, while varied shrinkage amplification factors were observed when the properties of the parent concrete and the RAC were different, i.e. larger shrinkage amplification factors for lower strength parent concrete and vice versa. For an RCA replacement ratio of 100%, the RCAs significantly influenced the 360-day drying shrinkage of the RAC by up to 27.6–59.6%. The variations in the κ_{sh} measurements induced by the different strengths of the parent concrete could not be accurately represented by the replacement ratio, physical properties (aggregate density or water absorption), or residual mortar content of the RCA. Additionally, the influence of the parent concrete service time (ranging from 1 year to 42 years) on the drying shrinkage of RAC was limited, with a maximum error of 8.4% in the 360-day measurements.

A new theoretical shrinkage model was proposed based on the two-phase composite material theory to account for the influence of parent concrete, by introducing two new parameters, namely, "$\kappa_{sh,a}$" to consider the effect of the residual mortar content and "$\kappa_{sh,f}$" to account for the difference in the shrinkage behaviour between the residual mortar and natural mortar. The proposed drying shrinkage model could describe the drying shrinkage of RAC with different concrete strengths reasonably well, with a mean value between the predicted and experimental values of κ_{sh} of 0.992, and a corresponding coefficient of variation of 9.10%.

Table A.1
Values for k_h.

Notional size h_0 (mm)	100	200	300	≥500
Size coefficient k_h	1.00	0.85	0.75	0.70

Further studies to investigate the influence of the parent concrete strength on the drying shrinkage of RAC, and the preconditions under which this influence is significant, are necessary. Moreover, further research is required to comprehensively evaluate the adequacy of the proposed shrinkage model and to further simplify the design expression.

Declaration of Competing Interest

The authors declare that they have no conflict of interest.

Acknowledgements

This study was funded by National Natural Science Foundation of China (51678195, 51808351), China; by Postdoctoral Research Plan of Heilongjiang (LBH-Q16098), by Open-funds of Key Lab of HIT (HITCE 201808), China; and by Liaoning Basic Scientific Plan (LJZ 2017021), China.

Appendix A

The drying shrinkage of natural concrete at t days could be predicted in accordance with Eq. (A.1) and composed of three parts: β_{ds} (t, t_s) describing the shrinkage development trend; $\varepsilon_{cd,0}$ representing the final drying shrinkage; and k_h referred to as the size coefficient depending on the notional size h_0 (mm), e.g. $h_0 = a/2$ for prism samples and $h_0 = d/2$ for cylinder samples.

$$\varepsilon_{cd}(t) = \beta_{ds}(t, t_s)\cdot\varepsilon_{cd,0}\cdot k_h \tag{A.1}$$

Part 1: β_{ds} (t, t_s) could be calculated by Eq. (A.2) and is independent of the relative humidity. $t - t_s$ is the drying time of test samples, with the beginning day of drying shrinkage referred to as t_s.

$$\beta_{ds}(t, t_s) = \frac{(t - t_s)}{(t - t_s) + 0.04\sqrt{h_0^3}} \tag{A.2}$$

Part 2: $\varepsilon_{cd,0}$ could be estimated via concrete strength (f_{cm}) and relative humidity RH, as shown in Eq. (A.3a)–(A.3b). α_{ds1} and α_{ds2} are the coefficients depending on the cement type, e.g. values of 4 and 0.12 specified for concrete using Class N cement.

$$\varepsilon_{cd,0} = 0.85\left[(220 + 110\cdot\alpha_{ds1}).\exp\left(-\alpha_{ds2}.\frac{f_{cm}}{10}\right)\right]\cdot 10^{-6}\cdot\beta_{RH} \tag{A.3a}$$

$$\beta_{RH} = 1.55\left[1 - \left(\frac{RH}{RH_0}\right)^3\right] \tag{A.3b}$$

Part 3: k_h could be estimated using the notional size h_0 (mm), and could easily obtained from Table A.1.

Appendix B. Supplementary material

Supplementary data to this article can be found online at https://doi.org/10.1016/j.engstruct.2019.109888.

References

[1] Hansen TC. Recycled aggregates and recycled aggregate concrete second state-of-the-art report developments 1945–1985. Mater Struct 1986;19(3):201–46. https://doi.org/10.1007/BF02472036.
[2] Xiao JZ, Li WG, Fan YH, Huang X. An overview of study on recycled aggregate concrete in China (1996–2011). Constr Build Mater 2012;31(2):364–83. https://doi.org/10.1016/j.conbuildmat.2011.12.074.
[3] Xiao JZ. Recycled aggregate concrete structures Berlin, Heidelbeg: Springer Tracts in Civ Eng; 2018. https://doi.org/10.1007/978-3-662-53987-3_16.
[4] Dobbelaere G, De Brito J, Evangelista L. Definition of an equivalent functional unit for structural concrete incorporating recycled aggregates. Eng Struct 2016;122(9):196–208. https://doi.org/10.1016/j.engstruct.2016.04.055.
[5] De Juan MS, Gutiérrez PA. Study on the influence of attached mortar content on the properties of recycled concrete aggregate. Constr Build Mater 2009;23(2):872–7. https://doi.org/10.1016/j.conbuildmat.2008.04.012.
[6] Butler L, West JS, Tighe SL. Effect of recycled concrete coarse aggregate from multiple sources on the hardened properties of concrete with equivalent compressive strength. Constr Build Mater 2013;47(10):1292–301. https://doi.org/10.1016/j.conbuildmat.2013.05.074.
[7] Corinaldesi V. Mechanical and elastic behaviour of concretes made of recycled-concrete coarse aggregates. Constr Build Mater 2010;24(9):1616–20. https://doi.org/10.1016/j.conbuildmat.2010.02.031.
[8] Geng Y, Wang YY, Chen J. Creep behaviour of concrete using recycled coarse aggregates obtained from source concrete with different strengths. Constr Build Mater 2016;128(12):199–213. https://doi.org/10.1016/j.conbuildmat.2016.10.086.
[9] Geng Y, Wang YY, Chen J. Time-dependent behaviour of steel tubular columns filled with recycled coarse aggregate concrete. J Constr Steel Res 2016;122(3):455–68. https://doi.org/10.1016/j.jcsr.2016.04.009.
[10] Wang QH, Ranzi G, Wang YY, Geng Y. Long-term behaviour of simply-supported steel-bars truss slabs with recycled coarse aggregate. Constr Build Mater 2016;116(6):335–46. https://doi.org/10.1016/j.conbuildmat.2016.04.150.
[11] Domingo-Cabo A, Lázaro C, López-Gayarre F, Serrano-López MA, Serna P, Castaño-Tabares JO. Creep and shrinkage of recycled aggregate concrete. Constr Build Mater 2009;23(7):2545–53. https://doi.org/10.1016/j.conbuildmat. 2009.02.018.
[12] Silva RV, de Brito J, Dhir RK. Comparative analysis of existing prediction models on the creep behaviour of recycled aggregate concrete. Eng Struct 2015;100(10):31–42. https://doi.org/10.1016/j.engstruct.2015.06.004.
[13] Recommendation RILEM. Specification for concrete with recycled aggregates. Mater Struct 1994;27(173):557. https://doi.org/10.1007/BF02473217.
[14] British Standard Institution. BS6543. Guide to the use of industrial by-products and waste materials in building and civil engineering, London, England; 1985.
[15] German Committee for Reinforced Concrete (DAfStb)-Code: Concrete with Recycled Aggregates; 1998.
[16] ACI Committee 555. ACI 555-01: removal and reuse of hardened concrete. American Concrete Institute, Farmington Hills; 2001.
[17] National Standard of the People's Republic of China. JCJ/T 240-2011. Technical specification for application of recycled aggregate; 2011 [in Chinese].
[18] National Standard of the People's Republic of China. DBJ/T 15-113. Technical specification for composite structures containing demolished concrete lumps; 2016 [in Chinese].
[19] National Standard of the People's Republic of China. CECS 2018. Technical specification for recycled-aggregate concrete-filled steel tubular structures; 2018 [in Chinese].
[20] Duan ZH, Poon CS. Properties of recycled aggregate concrete made with recycled aggregates with different amounts of old adhered mortars. Mater Des 2014;58(2):19–29. https://doi.org/10.1016/j.matdes.2014.01.044.
[21] Manzi S, Mazzotti C, Bignozzi MC. Short and long-term behavior of structural concrete with recycled concrete aggregate. Cem Concr Compos 2013;37:312–8. https://doi.org/10.1016/j.cemconcomp.2013.01.003.
[22] Wang YY, Wang QH, Ranzi G, Geng Y. Long-term behaviour of simply-supported composite slabs with recycled coarse aggregate. Mag Concr Res 2016;68(24):1278–93. https://doi.org/10.1016/j.conbuildmat.2016.04.150.
[23] Akbarnezhad A, Ong KCG, Tam CT, Zhang MH. Effects of the parent concrete properties and crushing procedure on the properties of coarse recycled concrete aggregates. J. Mater. Civ. Eng. 2013;25(12):1795–802. https://doi.org/10.1061/(ASCE)MT.1943-5533.0000789.
[24] Padmini AK, Ramamurthy K, Mathews MS. Influence of parent concrete on the properties of recycled aggregate concrete. Constr Build Mater 2009;23(2):829–36. https://doi.org/10.1016/j.conbuildmat.2008.03.006.
[25] Kou SC, Poon CS. Effect of the quality of parent concrete on the properties of high performance recycled aggregate concrete. Constr Build Mater 2015;77(12):501–8. https://doi.org/10.1016/j.conbuildmat.2014.12.035.

[26] Ravindrarajah RS, Tam CT. Properties of concrete made with crushed concrete as coarse aggregate. Mag Concr Res 1985;37(130):29–38. https://doi.org/10.1680/macr.1985.37.130.29.
[27] Wang YY, Chen J, Geng Y. Testing and analysis of axially loaded normal-strength recycled aggregate concrete filled steel tubular stub columns. Eng Struct 2015;86:192–212. https://doi.org/10.1016/j.engstruct.2015.01.007.
[28] Kiuchi T, Horiuchi E. An experimental study on recycle concrete by using high quality recycled coarse aggregate. Mem Fac Eng Osaka City Univ 2003;44:37–44.
[29] Tam VW, Wang K, Tam CM. Assessing relationships among properties of demolished concrete, recycled aggregate and recycled aggregate concrete using regression analysis. J Hazard Mater 2008;152(2):703–14. https://doi.org/10.1016/j. jhazmat.2007.07.061.
[30] Pepe M, Toledo Filho RD, Koenders EAB, Martinelli E. Alternative processing procedures for recycled aggregates in structural concrete. Constr Build Mater 2014;69:124–32. https://doi.org/10.1016/j.conbuildmat.2014.06.084.
[31] Omary S, Ghorbel E, Wardeh G. Relationships between recycled concrete aggregates characteristics and recycled aggregates concretes properties. Constr Build Mater 2016;108(4):163–74. https://doi.org/10.1016/j.conbuildmat.2016.01.042.
[32] Fathifazl G, Abbas A, Razaqpur AG, Isgor OB, Fournier B, Foo S. New mixture proportioning method for concrete made with coarse recycled concrete aggregate. J Mater Civil Eng 2009;21(10):601–11. https://doi.org/10.1061/(asce) 0899-1561(2009) 21:10(601).
[33] Tam VWY, Gao XF, Tam CM. Microstructural analysis of recycled aggregate concrete produced from two-stage mixing approach. Cem Concr Res 2005;35(6):1195–203. https://doi.org/10.1016/j.cemconres.2004.10.025.
[34] Xiao J, Li W, Sun Z. Properties of interfacial transition zones in recycled aggregate concrete tested by nanoindentation. Cem Concr Compos 2013;37(3):276–92. https://doi.org/10.1016/j.cemconcomp.2013.01.006.
[35] Kou SC, Poon CS, Agrela F. Comparisons of natural and recycled aggregate concretes prepared with the addition of different mineral admixtures. Cem Concr Compos 2011;33(8):788–95. https://doi.org/10.1016/j.cemconcomp. 2011.05.009.
[36] Ajdukiewicz A, Kliszczzewicz A. Influence of recycled aggregates on mechanical properties of HS/HPC. Cem Concr Compos 2002;24(2):269–79. https://doi.org/10.1016/S0958-9465(01)00012-9.
[37] Geng Y, Wang QH, Wang YY, Zhang H. Influence of service time of recycled coarse aggregate on the mechanical properties of recycled aggregate concrete. Mater Struct 2019. https://doi.org/10.1617/s11527-019-1395-0.
[38] Wang YY, Zhang H, Geng Y, Wang QH, Zhang SM. Prediction of the elastic modulus and the splitting tensile strength of concrete incorporating both fine and coarse recycled aggregate. Constr Build Mater 2019;215:332–46. https://doi.org/10.1016/j.conbuildmat.2019.04.212.
[39] Fathifazl G, Razaqpur AG, Isgor OB, Abbas A, Fournier B, Foo S. Shear capacity evaluation of steel reinforced recycled concrete (rrc) beams. Eng Struct 2011;33(3):1025–33. https://doi.org/10.1016/j.engstruct.2010.12.025.
[40] Abbas A, Fathifazl G, Isgor OB, Razaqpur AG, Fournier B, Foo S. Durability of recycled aggregate concrete designed with equivalent mortar volume method. Cem Concr Compos 2009;31(8):555–63. https://doi.org/10.1016/j. cemconcomp.2009.02.012.
[41] Silva RV, De Brito J, Dhir RK. Tensile strength behaviour of recycled aggregate concrete. Constr Build Mater 2015;83(5):108–18. https://doi.org/10.1016/j.conbuildmat.2015.03.034.
[42] Golafshani EM, Behnood A. Automatic regression methods for formulation of elastic modulus of recycled aggregate concrete. Appl Soft Comput 2018;64(3):377–400. https://doi.org/10.1016/j.asoc.2017.12.030.
[43] Deng F, He Y, Zhou S, Yu Y, Cheng H, Wu X. Compressive strength prediction of recycled concrete based on deep learning. Constr Build Mater 2018;175(6):562–9. https://doi.org/10.1016/j.conbuildmat.2018.04.169.
[44] Naderpour H, Rafiean AH, Fakharian P. Compressive strength prediction of environmentally friendly concrete using artificial neural networks. J Build Eng 2018;16(3):213–9. https://doi.org/10.1016/j.jobe.2018.01.007.
[45] Fathifazl G, Razaqpur AG, Isgor OB, Abbas A, Fournier B, Foo S. Creep and drying shrinkage characteristics of concrete produced with coarse recycled concrete aggregate. Cem Concr Compos 2011;33(10):1026–37. https://doi.org/10.1016/j.cemconcomp.2011.08.004.
[46] Geng Y, Zhao MZ, Hua Y, Wang YY. Creep model of concrete with recycled coarse and fine aggregates that accounts for creep development trend difference between recycled and natural aggregate concrete. Cem Concr Compos 2019;103:303–17. https://doi.org/10.1016/j.cemconcomp.2019.05.013.
[47] Seara-Paz S, González-Fonteboa Belén, Martínez-Abella Fernando, Carro-López Diego. Long-term flexural performance of reinforced concrete beams with recycled coarse aggregates. Const Build Mater 2018;176:593–607. https://doi.org/10.1016/j.conbuildmat.2018.05.069.
[48] Chen J, Wang Y, Roeder CW, Ma J. Behavior of normal-strength recycled aggregate concrete filled steel tubes under combined loading. Eng Struct 2017;130:23–40. https://doi.org/10.1016/j.engstruct.2016.09.046.
[49] Choi WC, Yun HD. Long-term deflection and flexural behavior of reinforced concrete beams with recycled aggregate. Mater Des 2013;51:742–50. https://doi.org/10.1016/j.matdes.2013.04.044.
[50] Ravindrarajah R, Tam CT. Recycled concrete as fine and coarse aggregates in concrete. Mag Concr Res 1987;39(141):214–20. https://doi.org/10.1680/macr.1987. 39.141.214.
[51] Maruyama I, Sato R. A trial of reducing autogenous shrinkage by recycled aggregate. Gaithersburg (MD), USA. In: Persson B, Bentz DP, Nilsson LO (Eds.), Proceedings of the 4th international seminar on self-desiccation and its importance in concrete technology; 2005. pp. 264–70.
[52] Tam VWY, Kotrayothar D, Xiao J. Long-term deformation behaviour of recycled aggregate concrete. Const Build Mater 2015;100:262–72. https://doi.org/10.1016/j.conbuildmat.2015.10.013.
[53] Sagoe-Crentsil KK, Brown T, Taylor AH. Performance of concrete made with commercially produced coarse recycled concrete aggregate. Cem Concr Res 2001;31(5):707–12. https://doi.org/10.1016/S0008-8846(00)00476-2.
[54] Gomez-Soberon, José MV. Relationship between gas adsorption and the shrinkage and creep of recycled aggregate concrete. Cem Concr Aggreg 2003;25(2):1–7. https://doi.org/10.1520/CCA10442J.
[55] Limbachiya M. Coarse recycled aggregates for use in new concrete. Eng Sustain. 2004;157(2):99–106. https://doi.org/10.1680/ensu.2004.157.2.99.
[56] Kou SC, Poon CS, Chan D. Influence of fly ash as a cement addition on the hardened properties of recycled aggregate concrete. Mater Struct 2008;41(7):1191–201. https://doi.org/10.1617/s11527-007-9317-y.
[57] Kou SC, Poon CS, Wan HW. Properties of concrete prepared with low-grade recycled aggregates. Constr Build Mater 2012;36(1):881–9. https://doi.org/10.1016/j.conbuildmat.2012.06.060.
[58] Castaño JO, Lopez-Gayarre F, Fernández CML. A study on drying shrinkage and creep of recycled concrete aggregate. Symposium of the international association for shell and spatial structures (50th. 2009. Valencia). Evolution and trends in design, analysis and construction of shell and spatial structures: proceedings; 2009.
[59] Gonzalez-Corominas A, Etxeberria M. Effects of using recycled concrete aggregates on the shrinkage of high performance concrete. Constr Build Mater 2016;115(4):32–41. https://doi.org/10.1016/j.conbuildmat.2016.04.031.
[60] Yang Sungchul, Lim Yujin. Mechanical strength and drying shrinkage properties of RCA concretes produced from old railway concrete sleepers using by a modified EMV method. Const Build Mater 2018;185:499–507. https://doi.org/10.1016/j.conbuildmat.2018.07.074.
[61] Silva RV, Brito JD, Dhir RK. Prediction of the shrinkage behavior of recycled aggregate concrete: a review. Constr Build Mater 2015;77:327–39. https://doi.org/10.1016/j.conbuildmat.2014.12.102.
[62] de Brito J, Robles R. Recycled aggregate concrete (RAC) methodology for estimating its long-term properties. Indian J Eng Mater S 2010;17(6):449–62. https://doi.org/10.1109/TPC.2010.2077851.
[63] de Brito J, Alves F. Concrete with recycled aggregates: the Portuguese experimental research. Mater Struct 2010;43(1):35–51. https://doi.org/10.1617/s11527 -010-9595-7.
[64] Katz A. Properties of concrete made with recycled aggregate from partially hydrated old concrete. Cem Concr Res 2003;33(5):703–11. https://doi.org/10.1016/S0008-8846(02)01033-5.
[65] Gholampour A, Ozbakkaloglu T. Time-dependent and long-term mechanical properties of concretes incorporating different grades of coarse recycled concrete aggregates. Eng Struct 2018;157:224–34. https://doi.org/10.1016/j.engstruct.2017.12.015.
[66] Pedro D, Brito JD, Evangelista L. Influence of the use of recycled concrete aggregates from different sources on structural concrete. Constr Build Mater 2014;71:141–51. https://doi.org/10.1016/j.conbuildmat.2014.08.030.
[67] Seara-Paz S, González-Fonteboa Belén, Martínez-Abella Fernando, Iris González-Taboada. Time-dependent behaviour of structural concrete made with recycled coarse aggregates. Creep and shrinkage. Const Build Mater 2016;122:95–109. https://doi.org/10.1016/j.conbuildmat.2016.06.050.
[68] Wang YY, Geng Y, Chang YC, Zhou CJ. Time-dependent behaviour of recycled concrete filled steel tubes using RCA from different parent waste material. Const Build Mater 2018;193:230–43. https://doi.org/10.1016/j.conbuildmat. 2018.10.201.
[69] Wang YY, Geng Y, Chen J, Zhao MZ. Testing and analysis on nonlinear creep behaviour of concrete-filled steel tubes with circular cross-section. Eng Struct 2019;86:26–46. https://doi.org/10.1016/j.engstruct.2019.01.065.
[70] Souche JC, Bendimerad A, Rozière Emmanuel, Salgues M, Devillers P, Garciadiaz E. Early age behaviour of recycled concrete aggregates under normal and severe drying conditions. J Build Eng 2017;13:244–53. https://doi.org/10.1016/j.jobe.2017.08.007.
[71] Cabral AEB, Schalch V, Dal Molin DCC, Ribeiro JLD, Ravindrarajah RS. Shrinkage modeling for recycled aggregate concretes. Rev IBRACON Estrut Mater 2010;3(1):1–23. https://doi.org/10.1590/S1983-41952010000100002.
[72] Wang YY, Wang QH, Geng Y. State-of-the-art of horizontal structural members using recycled aggregate concrete. Eng Mech 2018. https://doi.org/10.6052/j. issn.1000-4750.2017.06.ST10.
[73] National Standard of the People's Republic of China. JGJ-52-2006. Standard for technical requirements and test method of sand and crushed stone (or gravel) for ordinary concrete [in Chinese].
[74] National Standard of the People's Republic of China. JGJ 55-2011. Specification for mix proportion design of ordinary concrete [in Chinese].
[75] National Standard of the People's Republic of China. GB/T 50081-2002. Standard for test method of mechanical properties on ordinary concrete; 2002 [in Chinese].
[76] British Standards Institute. British Standard EN 12390-3. Testing HardenedConcrete. Part 3: compressive strength of test specimens. London, England; 2003.
[77] UNE-83316. Concrete tests. Determination of the modulus of elasticity in compression; 1996.
[78] National Standard of the People's Republic of China. GB/T 50082-2009. Standard for test methods of long-term performance and durability of ordinary concrete; 2009 [in Chinese].
[79] American Society for Testing Materials. ASTM C 157. Standard test method for drying shrinkage of concrete. Pennsylvania, USA; 2008.
[80] CEN European Committee for Standardization. Design of Concrete Structures, Part 1-1: general rules and rules for building. Eurocode 2; 2004.
[81] Neville, Adam M. Properties of concrete; 1973.